Research Square

Preprints are preliminary reports that have not undergone peer review.
They should not be considered conclusive, used to inform clinical practice,
or referenced by the media as validated information.

Digital Policy and Urban Climate Resilience: Unequal Adaptation Benefits across Chinese Cities

Zhen Tan
Bangor College, Central South University of Forestry and Technology
Yangxin Wang
Central China Normal University
Yaoyao Wang
t20162319@csuft.edu.cn

Bangor College, Central South University of Forestry and Technology

Article

Keywords: Digital policy, Extreme weather, Urban climate resilience, Adaptation inequality, Digital services

Posted Date: November 19th, 2026

DOI: https://doi.org/10.21203/rs.3.rs-11426723/v1

License: This work is licensed under a Creative Commons Attribution 4.0 International License.
Read Full License

Additional Declarations: No competing interests reported.

Word Count: 8,226 words (excluding references and figures).

Digital Policy and Urban Climate Resilience: Unequal Adaptation Benefits across Chinese Cities

Zhen Tan[1,†], Yangxin Wang[2,†], Yaoyao Wang[1,*]

[1] Bangor College, Central South University of Forestry and Technology, Changsha 410004, China

[2] School of Economics and Business Administration, Central China Normal University, Wuhan 430079, China

[*] Correspondence: Yaoyao Wang; t20162319@csuft.edu.cn

[†] Zhen Tan and Yangxin Wang contributed equally to this work.

Abstract

Extreme weather disrupts urban economic activity, but whether digital policy mitigates these losses and how its benefits are distributed remain unclear. Drawing on monthly nighttime-light and weather data for 283 Chinese cities from 2017 to 2025, this study evaluates the staggered Information Consumption Demonstration City programme using cohort-specific difference-in-differences estimates of weather sensitivity. Following designation, the estimated activity loss associated with one additional day of extreme heat or heavy rainfall is smaller by 0.00197 and 0.00263 log points, respectively. These buffering effects persist across alternative specifications but differ markedly between cities. Cities with stronger initial digital capacity obtain larger heat and rainfall buffers by 0.00143 and 0.00248 log points, respectively, than cities with weaker capacity. The differences persist under fixed population weighting. Policy designation also increases digital service adoption, which is positively associated with reduced weather sensitivity. Complementary machine-learning analyses identify nonlinear predictive relationships between weather exposure, past activity and local conditions. The findings suggest that digital policy can strengthen urban climate resilience while delivering uneven adaptation benefits, highlighting the importance of inclusive digital services in climate adaptation.

Keywords: Digital policy; Extreme weather; Urban climate resilience; Adaptation inequality; Digital services

1 Introduction

The severe rainfall in Henan in 2021 and the prolonged heatwave in the Yangtze River basin in 2022 substantially disrupted urban transport, production, and daily life. Heavy rainfall impeded mobility and deliveries, while persistent heat affected labor productivity, production schedules, and consumption. These events illustrate the continuing threat that extreme weather poses to urban economies and raise an important question: when weather shocks cannot be fully avoided, how can cities maintain economic continuity and strengthen their capacity to adapt?

The digital economy offers new ways for cities to respond to extreme weather. Digital payments, online transactions, and remote services reduce information and transaction costs, allowing some economic activities to continue when transport is disrupted or in-person services are restricted. However, these adaptation benefits may depend on existing infrastructure and service networks. Cities with stronger digital foundations generally have more developed transaction channels and service systems and can use

additional digital resources more effectively. Digital transformation may therefore affect both overall urban climate resilience and the distribution of adaptation benefits across cities.

China's Information Consumption Demonstration City program provides a policy setting in which to examine this issue. Since the relevant administrative measures took effect in 2019, cities have been designated in successive cohorts, creating variation in treatment timing. **Figure 1** shows the spatial distribution of the 283 candidate cities and 20 newly designated cities, together with new designations in each of the four cohorts. This setting allows a comparison of urban responses to extreme weather before and after digital development policies take effect.

Against this background, the study addresses three questions. First, can digital policy mitigate the adverse effects of extreme heat and heavy rainfall on urban economic activity? Second, do weather-buffering benefits differ across cities with different initial digital capacity, and do these differences persist under population weighting? Third, how are digital service adoption and initial city conditions related to economic activity during extreme weather?

To answer these questions, we integrate monthly nighttime lights, weather observations, and digital development data for 283 Chinese cities over 2017–2025. A cohort-specific weather-slope difference-in-differences model estimates the policy's weather-buffering effects. City grouping, fixed population weighting, and digital service channel analysis are used to examine the distribution of adaptation benefits. Interpretable machine learning complements this analysis by examining nonlinear predictive relationships among weather exposure, past activity, and initial city conditions.

The results show that designation as an Information Consumption Demonstration City significantly reduces urban activity losses associated with heat and heavy rainfall, although the adaptation benefits vary substantially across cities. Cities with stronger initial digital capacity experience greater weather buffering, and this advantage remains under fixed population weighting. Digital service adoption is positively associated with better adaptation performance, suggesting that pre-existing digital conditions influence how policy support translates into practical adaptive capacity.

The study makes three contributions. First, it evaluates digital policy through changes in weather sensitivity, extending research on the digital economy and urban climate resilience. Second, it incorporates differences in adaptation benefits across cities into policy evaluation, revealing a connection between initial digital capacity and the distribution of climate adaptation gains. Third, it combines policy evaluation with nonlinear predictive analysis to provide complementary evidence on urban economic performance during extreme weather. The findings inform urban policies that address climate adaptation and digital inclusion together.

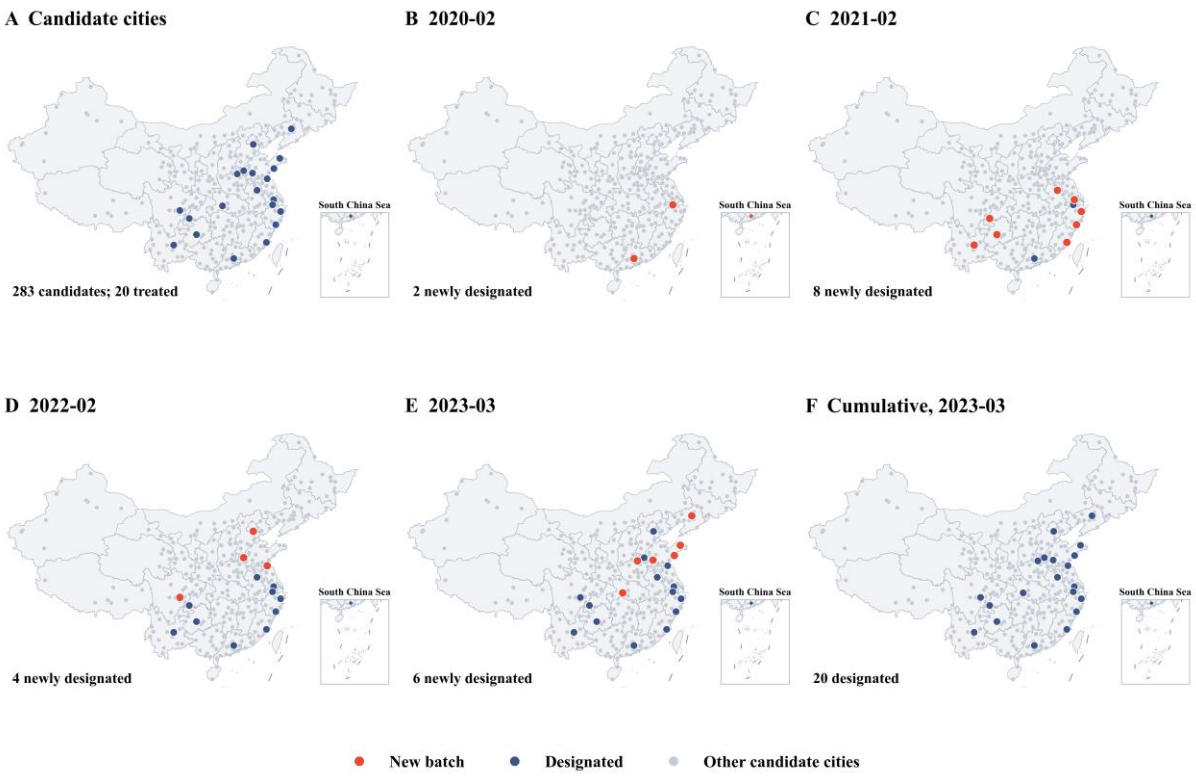


Figure 1 Staggered designation and spatial distribution of Information Consumption Demonstration Cities in China

Note: Panel A shows 283 candidate cities, including 20 treated cities. Panels B–E show new designations in the four cohorts (2, 8, 4, and 6 cities), and Panel F shows cumulative designations. Red, blue, and gray indicate newly designated, previously designated, and other candidate cities, respectively. Each map includes a South China Sea inset. The schematic base map uses DataV.GeoAtlas.

2 Theoretical background and research hypotheses

2.1 Weather shocks and urban adaptation

Extreme weather affects urban economies through labor supply, production efficiency, and market transactions. The economic consequences of climate shocks vary substantially across regions and exhibit nonlinear patterns. The relationship between temperature and economic output depends jointly on prevailing climatic conditions, development levels, and industrial structure (Carleton & Hsiang, 2016; Dell et al., 2014; Burke et al., 2015). Economic activity in different locations may respond differently to the same weather shock, reflecting the interaction between weather exposure and local adaptive capacity (Dell et al., 2012).

Labor and production are important channels through which weather affects urban economies. Heat can alter working time, reduce labor productivity, and affect firm output (Graff Zivin & Neidell, 2014; Somanathan et al., 2021). Temperature changes also affect manufacturing through firm productivity and resource allocation, while technologies that improve working conditions can reduce heat-related efficiency losses (Zhang et al., 2018; Adhvaryu et al., 2020). Rainfall shocks can increase transport, production scheduling, and service delivery costs; both changes in precipitation and exposure to extreme flooding have substantial economic consequences (Kotz et al., 2022; Dottori et al., 2018). Day-to-day temperature

variability also contains economic information beyond mean temperature, further illustrating the complex effects of weather shocks on economic activity (Kotz et al., 2021).

Urban responses to weather shocks also depend on the capacity to maintain economic continuity. Urban climate resilience involves dynamic processes through which interconnected socioeconomic systems maintain and restore their functions under external shocks. Resources, institutions, and the capacity to act jointly shape adaptation performance (Meerow et al., 2016; Siders, 2019). Local socioeconomic conditions influence the effectiveness of adaptation, and cities may respond through different combinations of production adjustment, resource coordination, and service substitution (Berrang-Ford et al., 2021). For urban economic systems, stronger adaptive capacity is reflected both in post-shock recovery and in smaller production, consumption, and transaction losses under comparable weather exposure.

Climate adaptation also has important distributional implications. The economic effects of extreme heat differ across income levels, while community recovery after natural disasters is closely related to socioeconomic conditions (Callahan & Mankin, 2022; Hong et al., 2021). Urban cooling resources and their benefits are also distributed unevenly across space (Li et al., 2024). A reduction in average weather losses therefore need not imply a narrower gap in adaptive capacity. Examining activity changes and buffering benefits across cities helps clarify both the economic and distributional effects of climate adaptation.

2.2 Digital policy and the distribution of benefits

By reducing the costs of information transmission, transaction organization, and market coordination, the digital economy creates new ways for cities to adapt to extreme weather. Digital technologies lower search, replication, transport, tracking, and verification costs, while their economic value also depends on changes in organizational processes, business models, and service delivery (Goldfarb & Tucker, 2019; Vial, 2019; Verhoef et al., 2021). When heat or heavy rainfall constrains in-person activity, online transactions, digital payments, and remote services can help firms and residents maintain some economic connections and reduce weather-related transaction disruptions.

Digital services can strengthen the ability to withstand external shocks by improving risk sharing and broadening the ways in which economic activity is organized. Mobile payments reduce transfer costs, helping households obtain outside support and sustain consumption (Jack & Suri, 2014; Suri & Jack, 2016). Remote and flexible work reduce the dependence of some activities on fixed workplaces, creating opportunities to adjust labor arrangements and maintain service continuity (Dingel & Neiman, 2020; Bloom et al., 2024). These channels allow digital technologies to substitute for some in-person activities when weather restrictions arise, increasing organizational flexibility in urban economies.

China's Information Consumption Demonstration City program promotes information consumption, digital service supply, and new application settings. It therefore provides an institutional context for studying the role of digital policy in climate adaptation. Digital development is related to urban economic resilience, while innovation, industrial structure, and human resources can influence how digital resources translate into adaptive capacity (Xu et al., 2024). Under extreme weather, digital policy may also reduce the sensitivity of urban economic activity to external shocks. As digital services enter routine transactions and

service processes, firms can coordinate orders, production, and deliveries more flexibly, while residents can use alternative channels to maintain some consumption. These adjustments support economic continuity.

The adaptation benefits of digital policy also depend on initial city conditions. Returns to information technology investment are closely linked to organizational change, and different information and communication technologies affect internal coordination and resource allocation in firms (Brynjolfsson & Hitt, 2000; Bloom et al., 2014). Digital technologies complement labor skills, so their benefits depend on human capital and the capacity to use them (Akerman et al., 2015). Local economic conditions also influence returns to internet technology and the distribution of associated employment opportunities (Forman et al., 2012; Hjort & Poulsen, 2019). Additional policy support may thus complement existing networks, technological applications, and organizational capacity, generating different adaptation benefits across cities.

Cities with stronger digital foundations generally have more mature payment systems, communication networks, and service platforms, enabling firms and residents to adopt new digital services at lower cost. When extreme weather constrains in-person transactions, well-developed networks help maintain information exchange, order coordination, and some service provision. Cities with weaker digital foundations may instead face constraints in network coverage, digital skills, and service accessibility. The digital divide concerns both infrastructure access and differences in use capabilities and realized benefits (Scheerder et al., 2017; van Deursen & van Dijk, 2019; Lythreatis et al., 2022). Digital policy may therefore improve average adaptation performance while producing benefit differences associated with pre-existing digital conditions.

2.3 Mechanisms and research hypotheses

The effects of digital policy on urban climate adaptation can be understood through transaction continuity, digital service adoption, and complementarity with initial conditions. First, heat and heavy rainfall increase the organizational costs of labor, production, and transactions. Digital technologies improve information coordination and expand alternative transaction channels, giving firms and residents greater flexibility to adjust economic activity. Digital policy may therefore promote routine activity and help cities maintain production, consumption, and service connections during adverse weather, reducing weather-related economic losses.

Second, digital service adoption links policy support to actual economic activity. Information consumption policy improves digital service supply and adoption conditions, allowing online payments, order management, information exchange, and remote services to become more widely integrated into urban economies. When weather constrains in-person transactions, digital services can support supply–demand coordination and partial service substitution, reducing interruptions to production and transactions. As digital applications spread, more flexible forms of service organization can strengthen economic continuity under external shocks.

Third, initial digital capacity affects the conversion of additional digital resources into adaptive capacity. Mature payment systems, communication networks, and user experience lower adoption costs and complement new policy support. Cities with stronger digital foundations may therefore obtain greater

weather-buffering benefits. Climate adaptation has clear spatial and social distributional dimensions, and the identity of beneficiaries and the distribution of benefits are important aspects of urban resilience evaluation (Shi et al., 2016; Meerow & Newell, 2019; Eriksen et al., 2021). Evaluating digital policy therefore requires considering average adaptation effects alongside differences across cities, including those associated with population size, historical weather exposure, and economic development.

Based on this reasoning, we develop a framework linking digital policy, digital service adoption, and urban weather adaptation. **Figure 2** summarizes the potential effects of policy on economic continuity and the connections between initial digital capacity, weather exposure, economic development, and the distribution of adaptation benefits. The empirical analysis first examines average weather buffering, then compares benefits across cities and evaluates the digital service channel. Interpretable machine learning provides complementary analysis of nonlinear predictive relationships between weather and initial city conditions.

We propose the following hypotheses:

H1: The Information Consumption Demonstration City program increases conditional urban economic activity and mitigates activity losses associated with extreme heat and heavy rainfall.

H2a: The Information Consumption Demonstration City program promotes digital service adoption.

H2b: Digital service adoption is positively associated with urban activity buffering under extreme heat and heavy rainfall.

H3a: Cities with stronger initial digital capacity obtain greater buffering benefits from extreme weather.

H3b: The relative buffering advantage of cities with stronger digital capacity persists under fixed registered-population weighting.

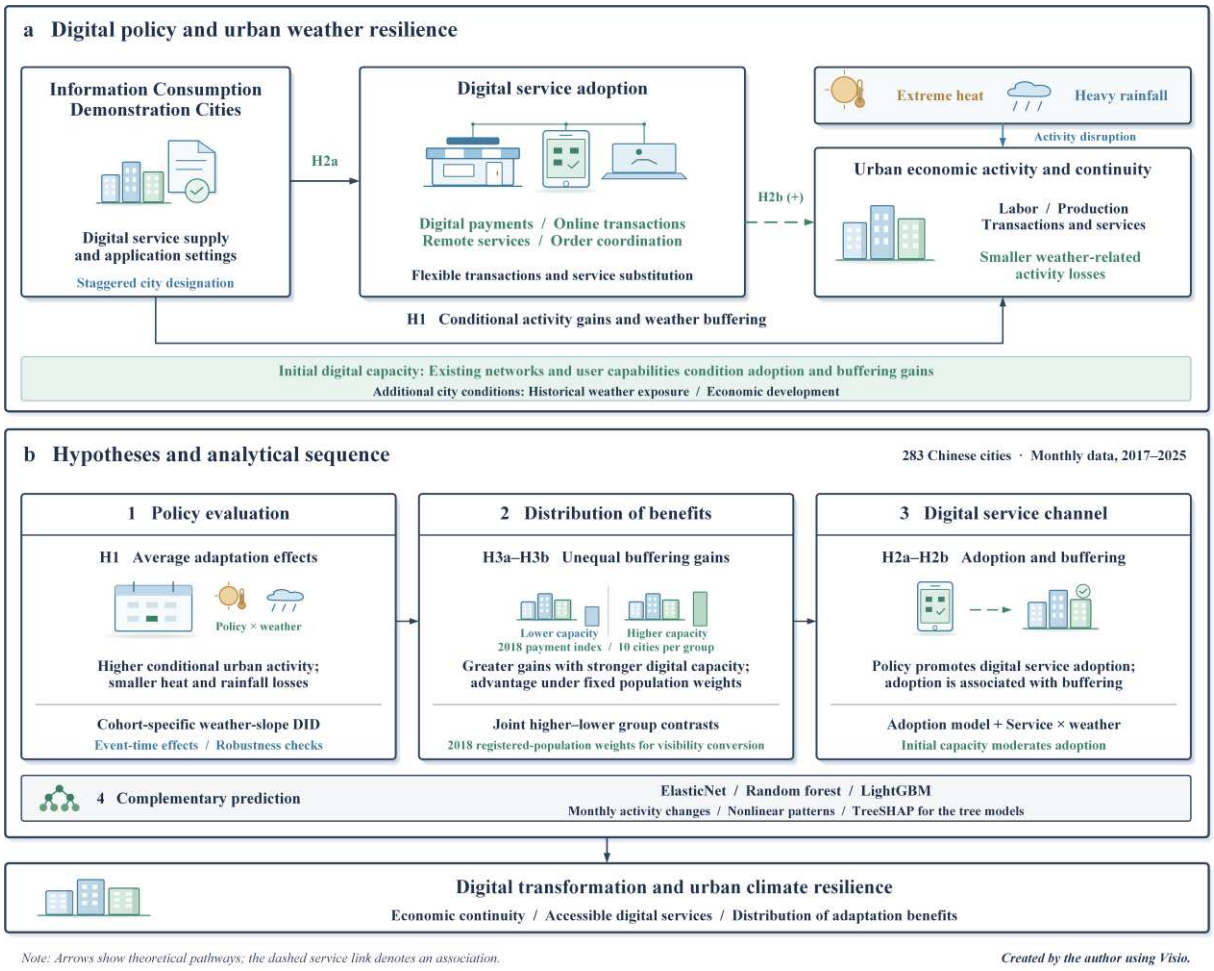


Figure 2 Theoretical framework and analytical sequence

Note: Panel A illustrates the weather-buffering and service adoption pathways. Panel B presents the sequence of policy evaluation, distributional analysis, and predictive interpretation. Arrows indicate theoretical relationships.

3 Research design and methods

3.1 Data and variables

The study uses the staggered designation of Information Consumption Demonstration Cities in China as its policy setting. Following the Administrative Measures for the Construction of Information Consumption Demonstration Cities (Trial), issued by the Ministry of Industry and Information Technology in 2019, and subsequent announcements, four cohorts entered the policy period in February 2020, February 2021, February 2022, and March 2023. Applying a first-designation rule and excluding cities with pre-existing demonstration status or inconsistent administrative coverage yields 20 treated cities, with 2, 8, 4, and 6 cities in the respective cohorts.

We combine nighttime lights, daily weather, digital finance, and city socioeconomic data into a monthly panel of 332 cities from April 2012 to December 2025, comprising 54,780 observations. The main study sample covers 283 cities over 2017–2025, with 30,564 city-month observations.

Nighttime lights provide a complementary measure of economic activity (Chen & Nordhaus, 2011; Henderson et al., 2012). We use NASA Black Marble monthly nighttime lights released through the World Bank's Space2Stats platform (Román et al., 2018) and apply the following logarithmic transformation:

$$Y_{it} = \ln(1 + NTL_{it}) \quad (1)$$

where NTL_{it} is the mean nighttime light intensity in city i in month t, and Y_{it} measures urban economic activity.

Weather data come from the NASA POWER/MERRA-2 daily meteorological database (Gelaro et al., 2017). Extreme heat days are days on which the daily maximum temperature exceeds the 95th percentile for the same calendar month in the 1981–2010 baseline. Heavy rain days are days on which precipitation exceeds the 95th percentile of all wet days in the baseline period; a wet day has at least 1 mm of precipitation:

$$H_{it} = \sum_{d \in t} \mathbf{1}\left(T_{id}^{\max} > Q_{i,m(d)}^{95}\right), \quad R_{it} = \sum_{d \in t} \mathbf{1}\left(P_{id} > Q_{i,\text{wet}}^{95}\right). \quad (2)$$

where H_{it} and R_{it} denote the monthly numbers of extreme heat days and heavy rain days, respectively.

The policy indicator D_{it} equals one from the month after a city's first designation announcement and zero beforehand. The digital baseline Z_i is constructed from the 2018 digital payment index, standardized within the 20 treated cities, and capped at ±1.5. The fixed visibility factor q_i is calculated from the 2018 mean of the original nighttime light activity measure and bounded at [0.035, 0.985]. Baseline controls include GDP per capita, broadband subscriptions, the digital payment index, and nighttime light quality. Extended specifications also include fiscal expenditure and registered population. The digital service variable M_{it} measures changes in city-level service use relative to a fixed baseline.

Table 1 summarizes the variables, measurements, and data sources.

Table 1 Main variable definitions, measurements, and data sources

Variable role	Variable	Definition and measurement	Source
Dependent variable	Urban activity Y	$\ln(1 + NTL)$, used to estimate policy effects and weather responses	World Bank Space2Stats / NASA Black Marble
Explanatory variable	Designation status D	Equals 1 from the month after first designation; pre-existing demonstration cities and cities with inconsistent administrative coverage are excluded under common rules	Ministry of Industry and Information Technology (MIIT): designation announcements and city lists
Explanatory variable	Extreme heat H	Days per month with maximum temperature above the same-calendar-month P95 threshold for 1981–2010	NASA POWER / MERRA-2 daily weather database
Explanatory variable	Heavy rainfall R	Days per month with rainfall above the P95 threshold of all baseline-period wet days	NASA POWER / MERRA-2 daily weather database
Explanatory variable	$D \times H$ and $D \times R$	Post-policy weather-slope differences; positive values indicate loss buffering	MIIT policy lists and NASA POWER; authors' calculations
Explanatory variable	Lags of H, R, and policy–weather interactions	Lags 1–3 of monthly weather and policy–weather interactions	NASA POWER weather data and MIIT policy lists; authors' construction
Control variable	GDP per capita	Standardized log GDP per capita in 2018	China City Statistical Yearbook, public compilation (CityEdu-Eco)
Control variable	Broadband subscriptions	2018 broadband subscriptions, transformed as $\ln(1 + x)$ and standardized	China City Statistical Yearbook, public compilation (CityEdu-Eco)
Control variable	Digital payments	Standardized 2018 digital payment index	Peking University Digital Financial Inclusion Index: payment subindex

Variable role	Variable	Definition and measurement	Source
Control variable	Nighttime light quality	Standardized mean monthly good-quality share in 2018	Space2Stats / Black Marble quality fields
Control variable	Fiscal expenditure and registered population	2018 fiscal expenditure and registered population, transformed as $\ln(1+x)$ and standardized	China City Statistical Yearbook, public compilation (CityEdu-Eco)
Mechanism variable	Digital services M	Deviation of the service-use index from the city-specific fixed baseline	Constructed from the China City Statistical Yearbook
Moderating variable	Digital payments Z	2018 payment index, standardized within 20 treated cities and capped at ±1.5	Peking University Digital Financial Inclusion Index: payment subindex
Measurement variable	Fixed visibility q	$1-\exp(-a_i)$, where a_i is the 2018 mean of the original activity measure; bounded at [0.035, 0.985]	Space2Stats / Black Marble; authors' calculations
Grouping variable	Higher/lower digital capacity	Fixed split at the median 2018 payment index of the 20 treated cities; the same threshold applies to comparison cities	Peking University Digital Financial Inclusion Index (2018 payment subindex); authors' grouping
Grouping variable	Weather exposure and development	Composite weather-exposure score for 2013–2018 and median GDP per capita in 2018	NASA POWER and CityEdu-Eco yearbook compilation; authors' grouping
Weight variable	Fixed registered-population weights	Registered population in 2018; normalized over treated cities with valid population data	CityEdu-Eco yearbook compilation: registered population in 2018

Note: Baseline controls are interacted with a linear time trend. Missing values are imputed using baseline medians across candidate cities, with missingness indicators included. Post-policy channel variables are excluded from the main model. Source names contain clickable links. CityEdu-Eco is a public compilation of the China City Statistical Yearbook.

3.2 Identification of policy effects

We begin with a two-way fixed effects (TWFE) model to examine how the Information Consumption Demonstration City program affects urban activity and sensitivity to extreme weather. Research on staggered treatment emphasizes the importance of comparison-group composition and response heterogeneity for estimation (Goodman-Bacon, 2021; Roth et al., 2023). We include interactions between policy status and weather shocks to identify the conditional activity-level effect and weather-buffering effects:

$$\begin{aligned} Y_{it} = {} & \alpha_{i,m(t)} + \lambda_{s(i),t} + q_i \xi_{s(i),t} \\ & + q_i[\beta D_{it} + \theta_H H_{it} + \theta_R R_{it} \\ & + \delta_H D_{it} H_{it} + \delta_R D_{it} R_{it} + \boldsymbol{L}_{it}^{\top} \gamma] + \varepsilon_{it}. \end{aligned} \tag{3}$$

where $\alpha_{i,m(t)}$ denotes city-by-calendar-month fixed effects, $\lambda_{s(i),t}$ denotes historical-policy-stratum-by-year-month fixed effects, and $q_i \xi_{s(i),t}$ controls for visibility differences with common time variation. $\boldsymbol{L}_{it}$ includes lags 1–3 of weather and policy–weather interactions, nonlinear tail terms, and baseline trend controls. β captures the conditional activity-level shift at zero weather exposure. δ_H and δ_R measure policy-related buffering of heat and heavy rainfall, respectively; positive coefficients indicate smaller weather-related activity losses.

Given the staggered designation of demonstration cities, and drawing on research on comparison groups and treatment-effect heterogeneity (Callaway & Sant'Anna, 2021; Sun & Abraham, 2021), we also use a cohort-specific weather-slope difference-in-differences (DID) model. Weather-buffering effects are estimated separately for each designation cohort and aggregated using fixed weights. Let g denote the cohort of first designation. The model is:

$$Y_{it}^{(g)} = \alpha_{i,m(t)}^{(g)} + \lambda_{s(i),t}^{(g)} + q_i \xi_{s(i),t}^{(g)} + q_i[\beta_g D_{it} + \theta_{Hg} H_{it} + \theta_{Rg} R_{it} + \delta_{Hg} D_{it} H_{it} + \delta_{Rg} D_{it} R_{it} + L_{it}^{(g)}] + \varepsilon_{it}^{(g)}. \quad (4)$$

where δ_{Hg} and δ_{Rg} are the heat and heavy rainfall buffering coefficients for cohort g, respectively, and $L_{it}^{(g)}$ collects the corresponding lag, tail, and trend controls. Each cohort uses a window from 36 months before designation to 23 months afterward. Months −12 to −3 form the reference period, and the two months immediately before designation are excluded. Comparison cities belong to the same historical policy stratum and remain untreated for at least two months after the window ends.

The weather-buffering coefficients for the four cohorts are aggregated using fixed weights based on the number of treated cities:

$$\hat{\bar{\delta}}_w = \sum_{g=1}^{4} \frac{n_g}{20} \overline{q}_g \hat{\delta}_{wg}, \qquad w \in \{H, R\}. \quad (5)$$

where n_g is the number of treated cities in a cohort and $\overline{q}_g$ is their mean visibility. The four cohort weights are 0.1, 0.4, 0.2, and 0.3, respectively. Standard errors are clustered by city (Cameron & Miller, 2015), and confidence intervals are constructed using 999 score-multiplier draws.

The dynamic analysis defines two annual pre-policy bins (months −36 to −25 and −24 to −13) and two annual post-policy bins (months 0–11 and 12–23) to examine changes in weather responses around implementation. Robustness checks use alternative weather thresholds, different policy windows, nighttime light quality screening, leave-one-cohort-out estimation, and pre-policy placebo dates. The interpretation of pre-policy responses draws on the discussion of parallel trends in Rambachan and Roth (2023).

3.3 Distribution of benefits and channels

To examine how weather-buffering benefits are distributed across cities, we split the 20 treated cities at the median of the 2018 digital payment index into higher- and lower-digital-capacity groups of 10 cities each. Group-specific weather responses are estimated jointly in the full candidate-city panel. The difference in buffering effects is defined as:

$$C_w = \overline{q}_1 \delta_{w1} - \overline{q}_0 \delta_{w0}, \qquad w \in \{H, R\}. \quad (6)$$

where subscripts 1 and 0 denote the higher- and lower-digital-capacity groups, respectively; δ_{w1} and δ_{w0} are the corresponding weather-buffering coefficients; and $\overline{q}_1$ and $\overline{q}_0$ are the mean visibility factors of treated cities in each group. The variance of the group difference is calculated from the covariance matrix of the joint regression:

$$\mathrm{Var}(\hat{C}_w) = \boldsymbol{L}\hat{\boldsymbol{\Sigma}}\boldsymbol{L}^{\top}. \quad (7)$$

where $\boldsymbol{L}$ is the linear contrast vector for the group difference and $\hat{\boldsymbol{\Sigma}}$ is the city-clustered covariance matrix of the jointly estimated coefficients.

We then use registered population in 2018 as fixed weights to calculate population-weighted visibility within each group:

$$\overline{q}_a^P = \frac{\sum_{i\in\mathcal{T}_a} P_{i,2018}\, q_i}{\sum_{i\in\mathcal{T}_a} P_{i,2018}}, \qquad a \in \{0,1\}. \tag{8}$$

where $P_{i,2018}$ denotes a city's registered population in 2018 and $\mathcal{T}_a$ is the set of treated cities in the corresponding digital group. Substituting population-weighted visibility into Equation (6) yields the buffering difference under a fixed population distribution. We also group cities by historical weather exposure over 2013–2018 and GDP per capita in 2018 to examine differences in adaptation benefits under other initial city conditions.

Digital service adoption is a potential channel through which digital policy affects urban weather responses. First, we use the deviation in digital service use, M_{it}, as the dependent variable to examine the effect of designation on adoption:

$$\begin{aligned} M_{it} = A_{i,m(t)} + B_{s(i),t} + q_i C_{s(i),t} \\ +\pi_0 D_{it} + \pi_Z D_{it} Z_i + e_{it}. \end{aligned} \tag{9}$$

where π_0 measures the change in digital service adoption associated with designation and π_Z captures how initial digital capacity moderates the policy response.

Second, we add digital services and their interactions with weather to the urban activity equation to examine the association between service adoption and extreme-weather responses:

$$\begin{aligned} Y_{it} = \mathrm{FE}_{it} + q_i X_{it}^{\top} b \\ +q_i[\eta M_{it} + \eta_H M_{it} H_{it} + \eta_R M_{it} R_{it}] + \varepsilon_{it}. \end{aligned} \tag{10}$$

where FE_{it} summarizes the fixed effects structure in Equation (3) and X_{it} includes the relevant policy, weather, and control variables. η measures the conditional association between digital services and activity, while η_H and η_R capture interactions between digital services and responses to heat and heavy rainfall, respectively.

Finally, we introduce triple interactions between initial digital capacity, policy status, and weather to examine the moderating role of the digital baseline:

$$\begin{aligned} Y_{it} = \mathrm{FE}_{it} + q_i X_{it}^{\top} b \\ +q_i[\psi_H Z_i H_{it} + \psi_R Z_i R_{it} \\ +\varphi_H Z_i D_{it} H_{it} + \varphi_R Z_i D_{it} R_{it}] + \varepsilon_{it}. \end{aligned} \tag{11}$$

where ψ_H and ψ_R control for differences in weather sensitivity associated with initial digital capacity, and φ_H and φ_R measure its moderating relationships with policy-related heat and rainfall buffering. The models include the corresponding lag terms and fixed effects to examine how service adoption and initial digital conditions relate to urban climate adaptation performance.

3.4 Machine learning analysis

Machine learning complements policy evaluation by describing nonlinear predictors of urban activity (Athey & Imbens, 2019; Mullainathan & Spiess, 2017).

ElasticNet, random forests (RF), and LightGBM model monthly activity changes through regularization, tree averaging, and gradient boosting (Breiman, 2001; Friedman, 2001; Zou & Hastie, 2005). The prediction target is:

$$\Delta Y_{it} = Y_{it} - Y_{i,t-1}. \tag{12}$$

All models share 29 features spanning weather, policy, initial digital conditions, geography, seasonality, and past activity. **Table A5** lists the features. ElasticNet estimates a linear relationship with combined L_1 and L_2 regularization, minimizing:

$$\min_{\boldsymbol{b}}\{\mathcal{L}(\boldsymbol{b}) + \alpha[\rho \parallel \boldsymbol{b} \parallel_1 + \frac{1-\rho}{2} \parallel \boldsymbol{b} \parallel_2^2]\}. \tag{13}$$

where $\mathcal{L}(\boldsymbol{b})$ is the squared-error loss, α is the regularization strength, and $\rho = 0.15$ is the mixing parameter.

RF averages regression trees, while LightGBM uses gradient boosting to fit nonlinear patterns:

$$\hat{f}_{\mathrm{RF}}(x) = \frac{1}{B}\sum_{b=1}^{B} T_b\,(x),$$
$$\hat{f}_{\mathrm{LGBM}}(x) = f_0(x) + \nu \sum_{k=1}^{K} T_k\,(x). \tag{14}$$

where B is the number of random forest trees, K is the number of boosting iterations, and ν is the learning rate. The final random forest uses 160 trees, while LightGBM uses 400 boosting iterations with a learning rate of 0.04. **Table A6** reports the full parameter settings.

The data are split chronologically into training (2019–2021), validation (2022–2023), and test (2024–2025) samples, containing 10,188, 6,792, and 6,792 observations, respectively. Parameters are selected using validation RMSE, and predictive performance is evaluated using RMSE, MAE, and R^2. A five-fold out-of-fold diagnostic, holding out provinces within the 2019–2023 development sample, also assesses prediction across regions.

For RF and LightGBM, TreeSHAP decomposes predictions into a baseline and feature contributions (Lundberg et al., 2020):

$$f(x_j) = \phi_0 + \sum_{k=1}^{p} \phi_{jk}. \tag{15}$$

where ϕ_0 is the baseline prediction and ϕ_{jk} is the contribution of feature k to the prediction for observation j. Global feature importance is calculated using mean absolute SHAP values:

$$I_k = \frac{1}{n}\sum_{j=1}^{n} |\phi_{jk}|. \tag{16}$$

We compare SHAP values on 1,200 shared test observations and construct dependence-curve intervals from 199 city-level bootstrap resamples.

We further select 400 observations from the common interpretation sample to calculate the full TreeSHAP interaction matrix. For distinct features k and l, the total pairwise interaction contribution is:

$$\psi_{kl} = 2\Phi_{kl}, \qquad k \neq l. \tag{17}$$

where Φ_{kl} is an off-diagonal TreeSHAP interaction element. We examine how weather interacts with digital payments and past activity in prediction.

4 Empirical results

4.1 Policy effects and weather buffering

4.1.1 Baseline regressions

Table 2 reports the effects of the Information Consumption Demonstration City program on urban economic activity and responses to extreme weather. In the main cohort-specific DID specification, the post-policy heat and heavy rainfall buffering coefficients are 0.00197 and 0.00263, respectively, and both are significantly positive. The conditional activity-level effect is 0.00981. The TWFE estimates and specifications with different baseline controls have consistent signs. These results indicate that digital policy improves urban activity and reduces weather-related activity losses, supporting H1.

Heat reduces opportunities for outdoor work and consumption, while heavy rainfall disrupts transport and delivery. Digital transactions provide alternative channels when in-person activity is constrained. The estimated reductions in weather sensitivity therefore capture an economic continuity benefit of digital policy beyond its effect on routine activity.

Table 2 Baseline regression results

Variable	(1) TWFE	(2) TWFE	(3) TWFE	(4) Cohort-slope DID	(5) Cohort-slope DID	(6) Cohort-slope DID
Dependent variable			Urban activity Y			
Policy level D	0.00800*** (0.00102)	0.00780*** (0.00099)	0.00782*** (0.00101)	0.00981*** (0.00104)	0.00985*** (0.00108)	0.00991*** (0.00109)
Heat $D \times H$	0.00223*** (0.00016)	0.00222*** (0.00015)	0.00222*** (0.00015)	0.00197*** (0.00012)	0.00197*** (0.00012)	0.00197*** (0.00012)
Rain $D \times R$	0.00313*** (0.00032)	0.00312*** (0.00032)	0.00312*** (0.00032)	0.00263*** (0.00027)	0.00263*** (0.00027)	0.00264*** (0.00027)
Heat H	-0.00466*** (0.00005)	-0.00466*** (0.00005)	-0.00466*** (0.00005)	-0.00468*** (0.00007)	-0.00468*** (0.00007)	-0.00467*** (0.00007)
Heavy rain R	-0.00676*** (0.00015)	-0.00671*** (0.00015)	-0.00670*** (0.00015)	-0.00658*** (0.00020)	-0.00657*** (0.00020)	-0.00658*** (0.00020)
$D \times H$ 95% CI	[0.00193, 0.00254]	[0.00192, 0.00253]	[0.00192, 0.00252]	[0.00173, 0.00220]	[0.00174, 0.00220]	[0.00173, 0.00221]
$D \times R$ 95% CI	[0.00250, 0.00376]	[0.00250, 0.00374]	[0.00250, 0.00375]	[0.00204, 0.00314]	[0.00204, 0.00314]	[0.00204, 0.00314]
GDP per capita trend	—	Included	Included	—	Included	Included
Broadband trend	—	Included	Included	—	Included	Included
Payment index trend	—	Included	Included	—	Included	Included
Light quality trend	—	Included	Included	—	Included	Included
Fiscal/population trends	—	—	Included	—	—	Included
Missingness trends	—	Included	Included	—	Included	Included
Weather lags and tails	Yes	Yes	Yes	Yes	Yes	Yes
City–calendar-month / stratum–time FE	Yes	Yes	Yes	Yes	Yes	Yes
Observations	30,564	30,564	30,564	58,116	58,116	58,116
Cities	283	283	283	283	283	283
Treated cities	20	20	20	20	20	20
Cohorts	4	4	4	4	4	4
Within R^2	0.737	0.738	0.738	—	—	—

Note: City-clustered standard errors are in parentheses. Coefficients are converted using the treated-city mean of q. Columns (1)–(3) use the full panel; Columns (4)–(6) use cohort-specific windows with 58,116 stacked comparison observations. Column (4) is the main specification. All specifications include fixed effects, weather lags, and tail terms. D represents the level shift at zero weather exposure. ***, **, and * indicate significance at the 1%, 5%, and 10% levels, respectively.

4.1.2 Dynamic effects

The adaptation effects of digital policy also vary over time. **Figure 3** shows no significant pre-policy trends in the heat or heavy rainfall response differences. During months 0–11 after designation, the buffering coefficients are 0.00132 and 0.00214, respectively, increasing to 0.00202 and 0.00318 in months 12–23. Both post-policy years exhibit positive buffering, with stronger estimated effects in the second year, providing further support for H1.

Buffering strengthens after designation, consistent with the gradual integration of payments, online transactions, and digital service platforms into everyday activity. Lag estimates concentrate benefits in the shock month and shortly thereafter, when alternative coordination channels are most valuable. **Tables A1 and A4** report the event-bin and short-run lag estimates.

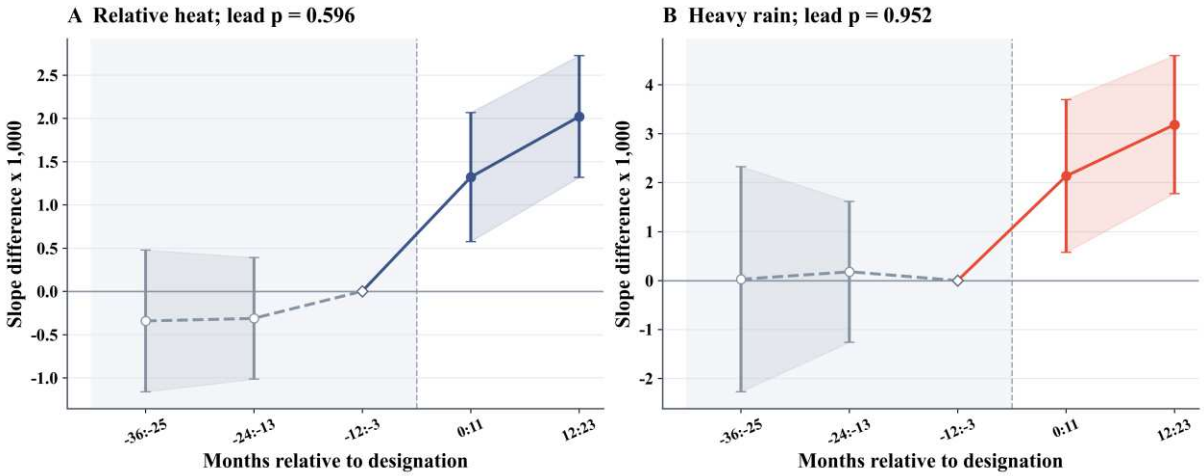


Figure 3 Parallel-trend diagnostics and annual weather-buffering effects

Note: Panels A and B show heat and heavy rainfall, respectively. The reference period is months −12 to −3. Gray hollow markers denote leads, colored markers denote post-policy responses, and diamonds denote the zero reference. Shading and error bars show 95% simultaneous intervals within each weather family, constructed using 999 city-level score-multiplier draws.

4.1.3 Robustness checks

Table 3 and **Figure 4** examine the main findings under alternative settings. All 10 specifications yield positive heat and heavy rainfall buffering when weather thresholds, policy windows, and nighttime light samples are changed and designation cohorts are sequentially excluded. In the high-quality nighttime light sample, the two buffering coefficients are 0.00256 and 0.00298, respectively. Pre-policy placebo-date tests also reveal no significant spurious policy responses.

Positive buffering persists under broader and stricter weather thresholds, different policy windows, and cohort exclusions. Placebo-date tests show no significant spurious pre-policy effects. This stability supports H1 and suggests that transaction flexibility contributes to weather adaptation. **Table A2** reports the lead and placebo diagnostics.

Table 3 Robustness checks

Variable	Specification	Specification	Specification	Specification	Specification
Panel A	**(1) Main**	**(2) 6-month post**	**(3) P90**	**(4) P99**	**(5) 35°C/50mm**
Heat $D \times H$	0.00197*** (0.00012)	0.00116*** (0.00025)	0.00132*** (0.00013)	0.00285*** (0.00038)	0.00053*** (0.00016)
Rain $D \times R$	0.00263*** (0.00027)	0.00304*** (0.00061)	0.00203*** (0.00021)	0.00418*** (0.00087)	0.00311** (0.00120)
Heat 95% CI	[0.00173, 0.00220]	[0.00067, 0.00165]	[0.00107, 0.00157]	[0.00211, 0.00360]	[0.00023, 0.00084]
Rain 95% CI	[0.00204, 0.00314]	[0.00190, 0.00419]	[0.00160, 0.00246]	[0.00246, 0.00575]	[0.00078, 0.00546]
Stacked observations	58,116	40,960	58,116	58,116	58,116
Cities	283	283	283	283	283
Treated cities	20	20	20	20	20
Panel B	**(6) Quality screen**	**(7) Omit 2020**	**(8) Omit 2021**	**(9) Omit 2022**	**(10) Omit 2023**
Heat $D \times H$	0.00256*** (0.00028)	0.00183*** (0.00013)	0.00164*** (0.00013)	0.00219*** (0.00014)	0.00219*** (0.00015)
Rain $D \times R$	0.00298*** (0.00115)	0.00243*** (0.00030)	0.00203*** (0.00035)	0.00297*** (0.00028)	0.00302*** (0.00032)
Heat 95% CI	[0.00203, 0.00307]	[0.00159, 0.00209]	[0.00139, 0.00188]	[0.00194, 0.00247]	[0.00189, 0.00248]
Rain 95% CI	[0.00072, 0.00508]	[0.00180, 0.00302]	[0.00137, 0.00271]	[0.00240, 0.00351]	[0.00238, 0.00362]
Stacked observations	20,021	45,124	42,398	44,312	42,514
Cities	279	281	275	279	280
Treated cities	19	18	12	16	14

Note: City-clustered standard errors are in parentheses. The 95% intervals are based on 999 score-multiplier draws. Coefficient units differ across weather thresholds. ***, **, and * indicate significance at the 1%, 5%, and 10% levels, respectively.

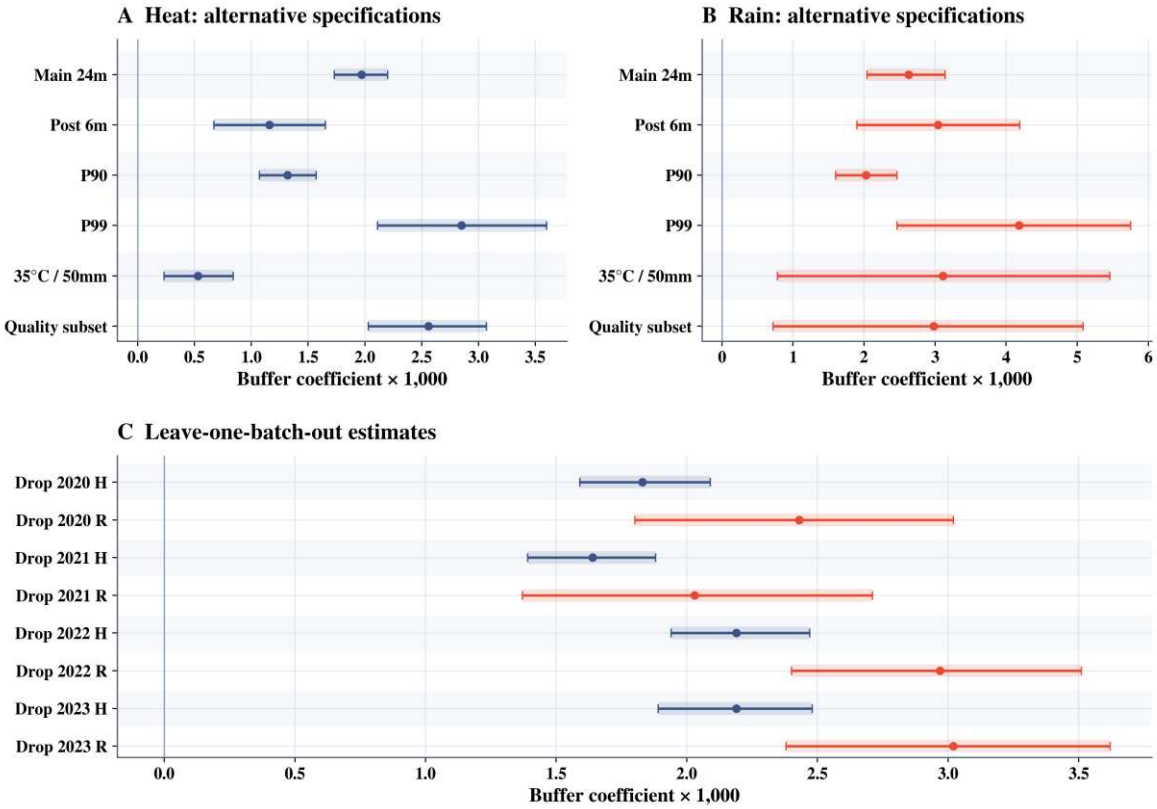


Figure 4 Alternative specifications and cohort influence

Note: Panels A and B show alternative specifications for heat and heavy rainfall, respectively, with 95% pointwise score-multiplier intervals. Panel C shows leave-one-cohort-out estimates.

4.2 Distribution of adaptation benefits

4.2.1 Differences by initial digital capacity

Improved average weather buffering does not imply equal adaptation benefits for all cities. **Table 4** shows a heat-buffering coefficient of 0.00259 for cities with higher initial digital capacity and 0.00116 for those with lower capacity, yielding a difference of 0.00143. The corresponding heavy rainfall coefficients are 0.00409 and 0.00161, a difference of 0.00248. Both weather-buffering differences are significantly positive. The group difference in the general conditional activity-level effect is insignificant, suggesting that the digital advantage is primarily reflected in protection of activity during adverse weather. This finding supports H3a.

Stronger digital payment and communication networks may lower the cost of substituting online services for interrupted in-person transactions. Although both groups receive policy support, differences in coverage and use can affect how quickly firms and residents adjust. This complementarity helps explain why higher-capacity cities obtain larger buffering gains.

Table A3 reports the digital-group samples and fixed weights.

Table 4 Initial digital capacity and the distribution of buffering benefits

Variable	(1) Lower digital	(2) Higher digital	(3) Difference
Panel A Equal city weights	**Lower digital**	**Higher digital**	**Higher − lower**
Heat $D \times H$	0.00116*** (0.00016)	0.00259*** (0.00019)	0.00143*** (0.00024)
Rain $D \times R$	0.00161*** (0.00033)	0.00409*** (0.00031)	0.00248*** (0.00046)
Heat p	<0.001	<0.001	<0.001
Rain p	<0.001	<0.001	<0.001
Treated cities	10	10	20
Panel B Fixed registered-population weights	**Lower digital**	**Higher digital**	**Higher − lower**
Heat $D \times H$	0.00117*** (0.00016)	0.00270*** (0.00020)	0.00154*** (0.00025)
Rain $D \times R$	0.00163*** (0.00034)	0.00427*** (0.00033)	0.00264*** (0.00047)
Heat p	<0.001	<0.001	<0.001
Rain p	<0.001	<0.001	<0.001
Treated cities with population data	10	10	20

Note: The treated cities are split at the median of the 2018 payment index into two groups of 10. Group-difference estimates incorporate within-city covariance. Panel B uses fixed 2018 registered-population weights to convert group-specific mean q; population data are available for all 20 treated cities. ***, **, and * indicate significance at the 1%, 5%, and 10% levels, respectively.

4.2.2 Population-weighted differences

Figure 5 compares adaptation benefits under equal city weights and fixed population weights. With weights based on registered population in 2018, the heat and heavy rainfall buffering advantages of higher-digital-capacity cities are 0.00154 and 0.00264, respectively, and both are significantly positive. These findings are consistent with the equally weighted estimates and support H3b.

Fixed population weighting incorporates city population size into the assessment of average buffering benefits, allowing differences to be evaluated under a given population distribution. The advantage of cities with stronger digital foundations persists after this adjustment, indicating that the unequal distribution of adaptation benefits is relatively stable.

This finding also highlights the distributional dimension of digital policy. Mature digital service networks help cities use policy resources more effectively, whereas cities with weaker initial conditions may require additional complementary investment to obtain comparable benefits. Alongside improvements in overall urban climate resilience, better service accessibility in areas with weak digital foundations is important for extending the reach of digital adaptation benefits.

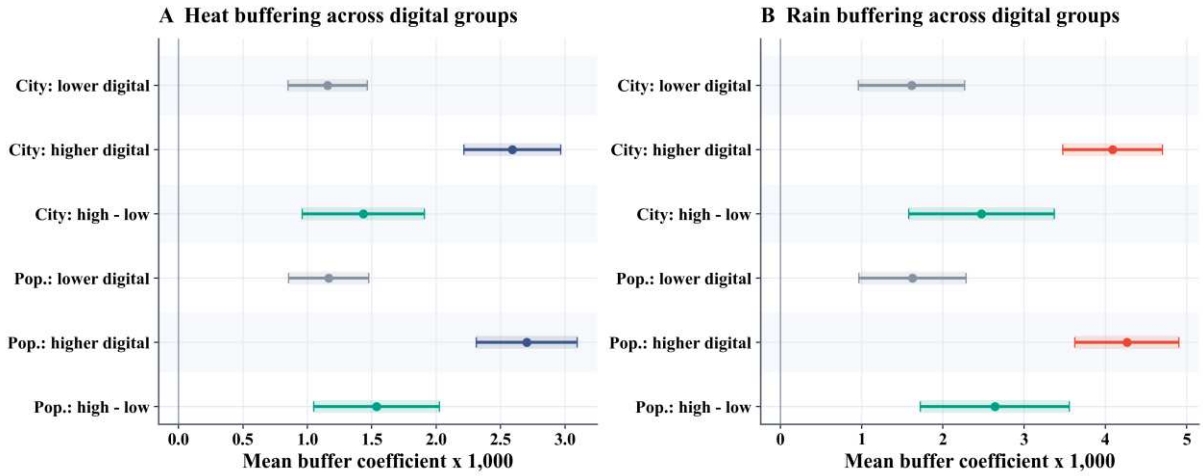


Figure 5 Weather buffering by digital capacity under equal city and fixed population weights

Note: Panels A and B show heat and heavy rainfall, respectively. Each panel reports within-group buffering and higher-minus-lower differences under equal city weights and fixed 2018 registered-population weights. Line segments show city-clustered 95% intervals; differences incorporate within-city covariance.

4.3 Service channels and heterogeneity

4.3.1 Digital service channel

The effects of digital policy on weather responses depend on whether digital services enter actual economic activity. **Table 5** shows that designation significantly promotes digital service adoption, with a policy coefficient of 0.06998 and an interaction coefficient between policy and initial digital capacity of 0.02342. **Figure 6A** also shows substantial increases in service adoption in both post-policy years. These findings suggest that demonstration city development encourages actual use of digital services, supporting H2a.

Digital services offer alternative means of arranging orders and transactions during weather disruptions. The interactions of service use with heat and heavy rainfall are 0.01740 and 0.02737, respectively, and are significantly positive. **Figure 6B** shows corresponding positive associations, consistent with H2b. These estimates describe conditional relationships rather than separately identified causal mediation.

Initial digital capacity also moderates weather buffering: the heat and rainfall triple-interaction estimates are 0.00099 and 0.00176. Both are positive, consistent with mature service networks helping cities benefit from digital policy. Adoption and baseline capacity jointly clarify the uneven distribution of adaptation gains.

Table 5 Mechanism analysis

Variable	(1) Service adoption	(2) Channel association	(3) Digital moderation
Dependent variable	Digital services M	Urban activity Y	Urban activity Y
Policy D	0.06998*** (0.00113)	—	—
$D \times Z$	0.02342*** (0.00090)	—	—
Services M	—	0.07198*** (0.00770)	—
$M \times H$	—	0.01740*** (0.00175)	—
$M \times R$	—	0.02737*** (0.00402)	—
$D \times H \times Z$	—	—	0.00099*** (0.00018)
$D \times R \times Z$	—	—	0.00176*** (0.00039)
Fixed effects	Yes	Yes	Yes
Observations	30,564	30,564	30,564
Cities	283	283	283

Note: City-clustered standard errors are in parentheses. The D term in the service equation is not multiplied by q. Activity equations report structural coefficients adjusted for q, without conversion using the treated-city mean of q. Channel estimates represent conditional associations. ***, **, and * indicate significance at the 1%, 5%, and 10% levels, respectively.

4.3.2 Heterogeneity in city conditions

Historical weather exposure and economic development also influence urban adaptive capacity. **Table 6** and **Figure 6C–D** show that cities with higher historical exposure have heat and heavy rainfall buffering effects that exceed those of low-exposure cities by 0.00073 and 0.00136, respectively. The rainfall difference is significant at the 5% level. Grouping cities by economic development yields heat and rainfall buffering advantages of 0.00178 and 0.00279 for higher-GDP-per-capita cities, and both differences are significantly positive.

These differences reflect the connection between adaptive capacity and existing economic resources. More developed cities generally have better infrastructure, market services, and organizational capacity and can use more resources to maintain economic activity during extreme weather. Cities that have historically experienced more weather shocks do not necessarily possess comparable economic adjustment capacity.

Together, the group comparisons show that adaptation depends on economic resources and digital networks as well as weather exposure. This reinforces the role of initial conditions in H3a.

Table 6 Heterogeneity by weather exposure and economic development

Variable	(1) Lower exposure	(2) Higher exposure	(3) Lower GDP	(4) Higher GDP
Panel A Group-specific slopes				
Heat $D \times H$	0.00189*** (0.00036)	0.00261*** (0.00017)	0.00068*** (0.00009)	0.00246*** (0.00017)
Rain $D \times R$	0.00247*** (0.00049)	0.00384*** (0.00046)	0.00071*** (0.00021)	0.00350*** (0.00034)
Treated cities	13	7	4	16
Cities	283	283	283	283
Observations	30,564	30,564	30,564	30,564
Panel B Higher-minus-lower differences				
Heat difference	0.00073* (0.00039)	0.00073* (0.00039)	0.00178*** (0.00018)	0.00178*** (0.00018)
Rain difference	0.00136** (0.00068)	0.00136** (0.00068)	0.00279*** (0.00041)	0.00279*** (0.00041)
Heat difference p	0.062	0.062	<0.001	<0.001
Rain difference p	0.045	0.045	<0.001	<0.001

Note: Exposure groups use the 2013–2018 composite weather score; development groups use 2018 GDP per capita. Treated-city counts are 13/7 for lower/higher exposure and 4/16 for lower/higher GDP. Differences incorporate within-city covariance. Panel B repeats each difference in the corresponding pair of columns. ***, **, and * indicate significance at the 1%, 5%, and 10% levels, respectively.

Figure 6 summarizes digital service adoption, its association with weather responses, and buffering differences across city conditions. The positive connection between service use and weather buffering provides linked evidence for H2a and H2b. Differences by digital capacity and economic development further reveal the distribution of urban adaptation benefits.

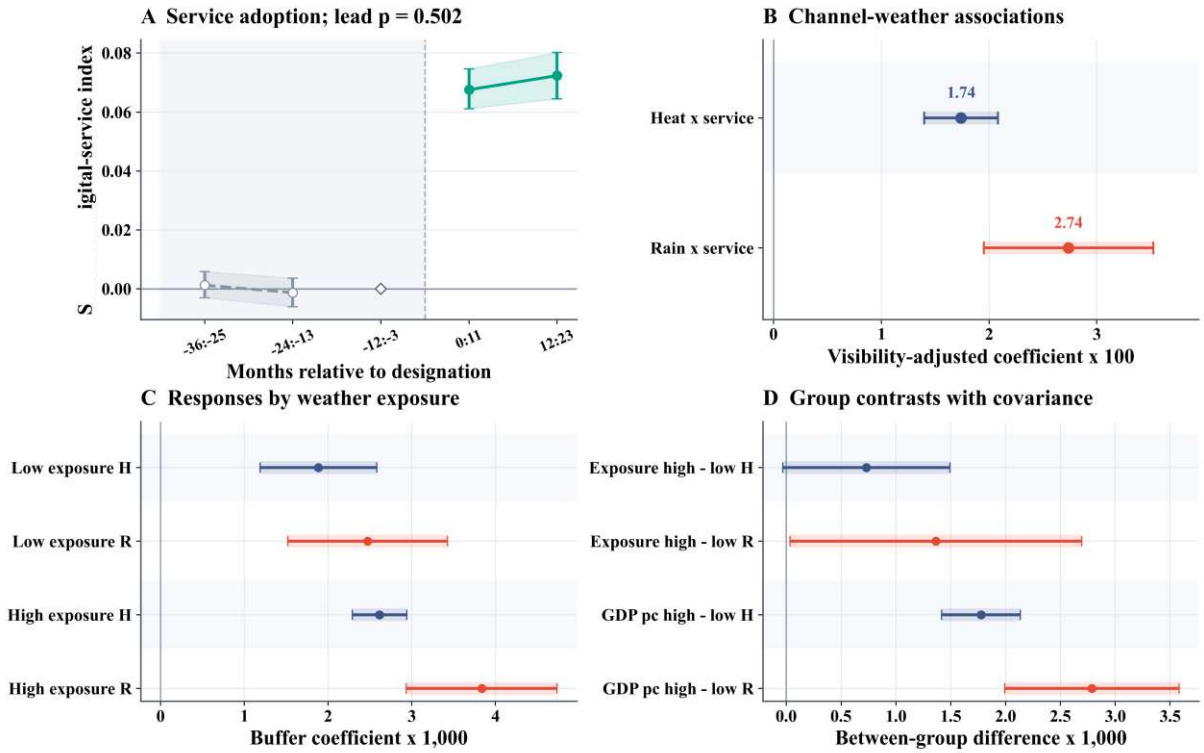


Figure 6 Digital service channels and heterogeneity in local conditions

Note: Panel A shows the dynamics of service adoption with 95% pointwise score-multiplier intervals. Panel B shows service–weather associations, Panel C reports weather-exposure groups, and Panel D shows differences by exposure and GDP. Panels B–D use city-clustered 95% intervals. H/R denotes heat/heavy rainfall. Scales are reported in **Tables 5–6**.

4.4 Machine learning results

4.4.1 Predictive performance

Building on the policy and distributional analyses, we use machine learning to examine complex relationships in monthly urban activity changes. **Table 7** shows that LightGBM achieves an out-of-time test R^2 of 0.5182 in 2024–2025, exceeding ElasticNet (0.4740) and RF (0.3962). ElasticNet performs better in the province-held-out evaluation, indicating that the models' ability to capture urban activity patterns varies across prediction tasks.

Temporal and provincial evaluations indicate that nonlinear models can help explain short-run activity fluctuations, while linear regularization transfers more effectively across provinces.

Table 7 Predictive performance of machine learning models

Metric	(1) ElasticNet	(2) RF	(3) LightGBM
Temporal validation 2022–2023			
RMSE	0.01525	0.01951	0.01619
MAE	0.01069	0.01346	0.01119
R^2	0.6787	0.4745	0.6379
N	6,792	6,792	6,792
Temporal test 2024–2025			
RMSE	0.02236	0.02396	0.02140
MAE	0.01538	0.01591	0.01445
R^2	0.4740	0.3962	0.5182
N	6,792	6,792	6,792
Development sample: five-fold province OOF			
RMSE	0.01458	0.01872	0.01629
MAE	0.01033	0.01295	0.01120
R^2	0.6756	0.4647	0.5946
N	16,980	16,980	16,980

Note: The target is the monthly change in urban activity. Parameters are selected using only the temporal validation sample. OOF refers to five-fold province-held-out diagnostics within the 2019–2023 development sample. Imputation and standardization are fitted separately within each fold, using the previously selected parameters.

4.4.2 Global feature contributions

Figure 7 shows that past activity, seasonality, and weather dominate predictive contributions in both tree models. Activity lags of one and twelve months are especially prominent; policy status and baseline digital capacity contribute relatively little.

Activity lags and seasonality capture routine production and consumption patterns, while weather helps predict departures from those patterns.

These rankings complement policy estimates of weather sensitivity rather than measuring causal effects of individual predictors.

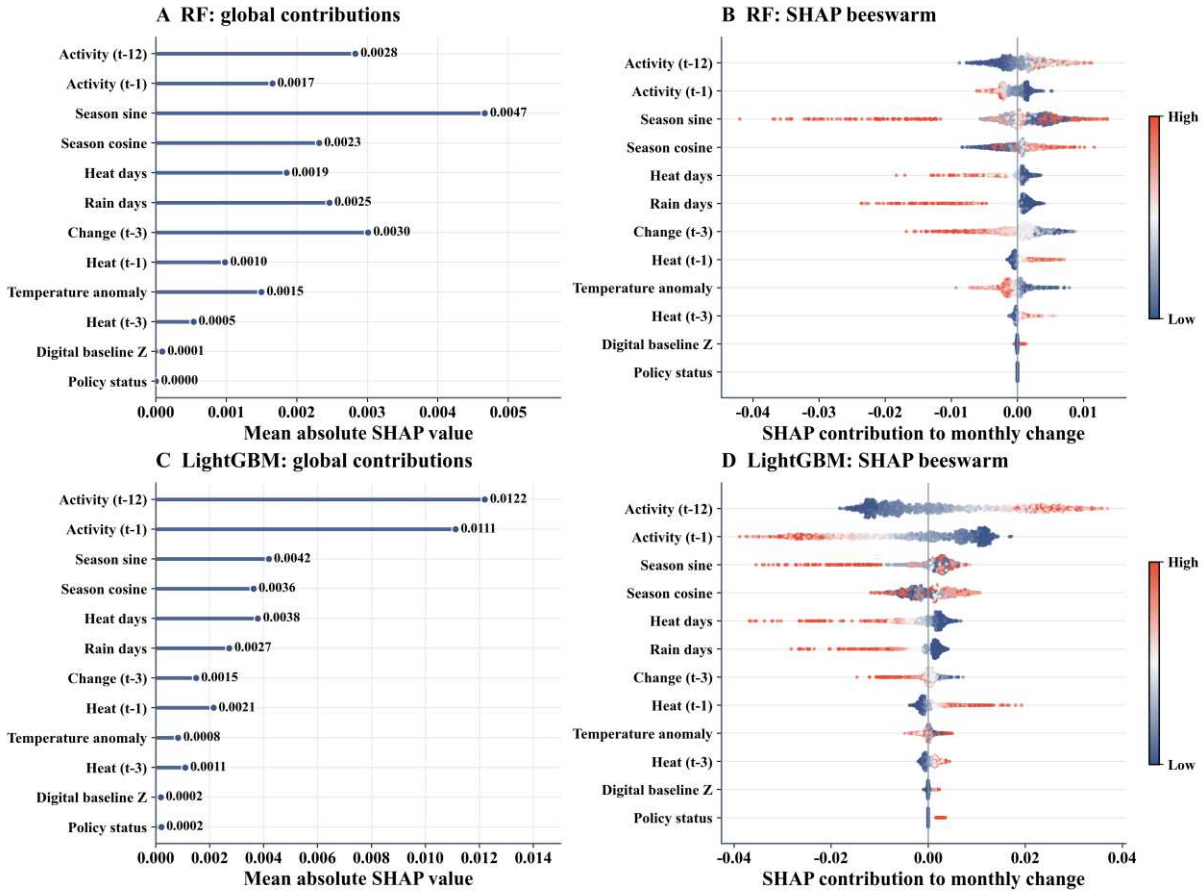


Figure 7 Contributions and SHAP distributions for monthly activity changes across two models

Note: Panels A–B show RF and Panels C–D show LightGBM. The left column reports mean absolute contributions, and the right column shows beeswarm distributions. Both models use the same 1,200 test observations and feature order. Blue to red indicates low to high feature values.

4.4.3 Nonlinear dependence

Figure 8 shows nonlinear SHAP dependence on current and lagged heat and rainfall, with contributions changing across exposure levels.

Changes in work schedules, transport, and delivery may sustain activity under moderate exposure, whereas severe conditions can constrain such adjustments. These dependence curves indicate exposure-specific predictive patterns.

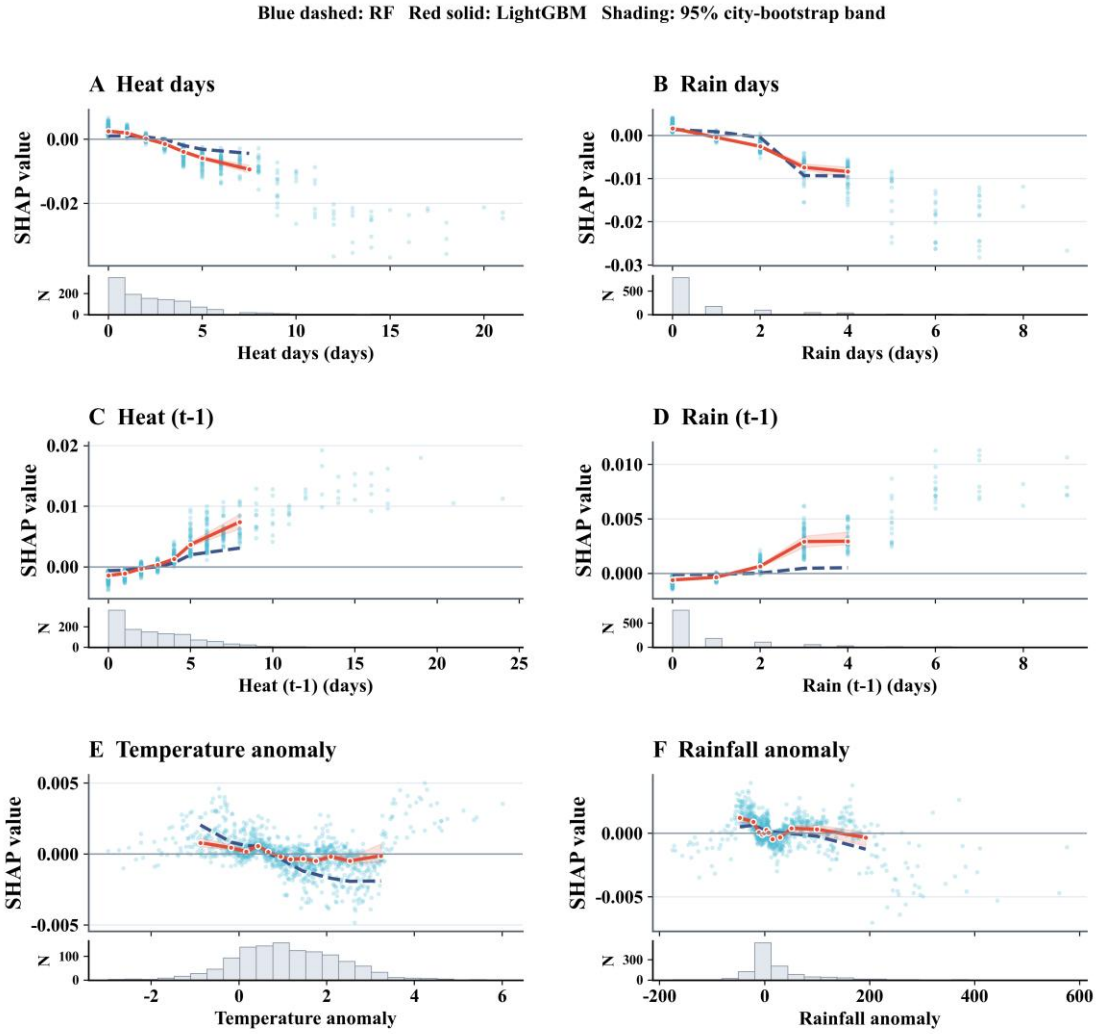


Figure 8 SHAP dependence for weather shocks and short-run persistence

Note: Panels A–F show heat, heavy rainfall, their first lags, and temperature and rainfall anomalies, respectively. Points are LightGBM contributions. Blue dashed and red solid lines show binned medians for RF and LightGBM. Shading shows 95% bands from 199 city-level bootstrap resamples with the models held fixed. The lower strips show sample distributions; each bin contains at least 20 observations.

Figure 9 shows nonlinear dependence on past activity, digital payments, broadband subscriptions, and GDP per capita. Historical activity captures persistence, while digital and economic conditions add information about local capacity.

These features highlight the combined role of recent activity and pre-existing city conditions in short-run prediction.

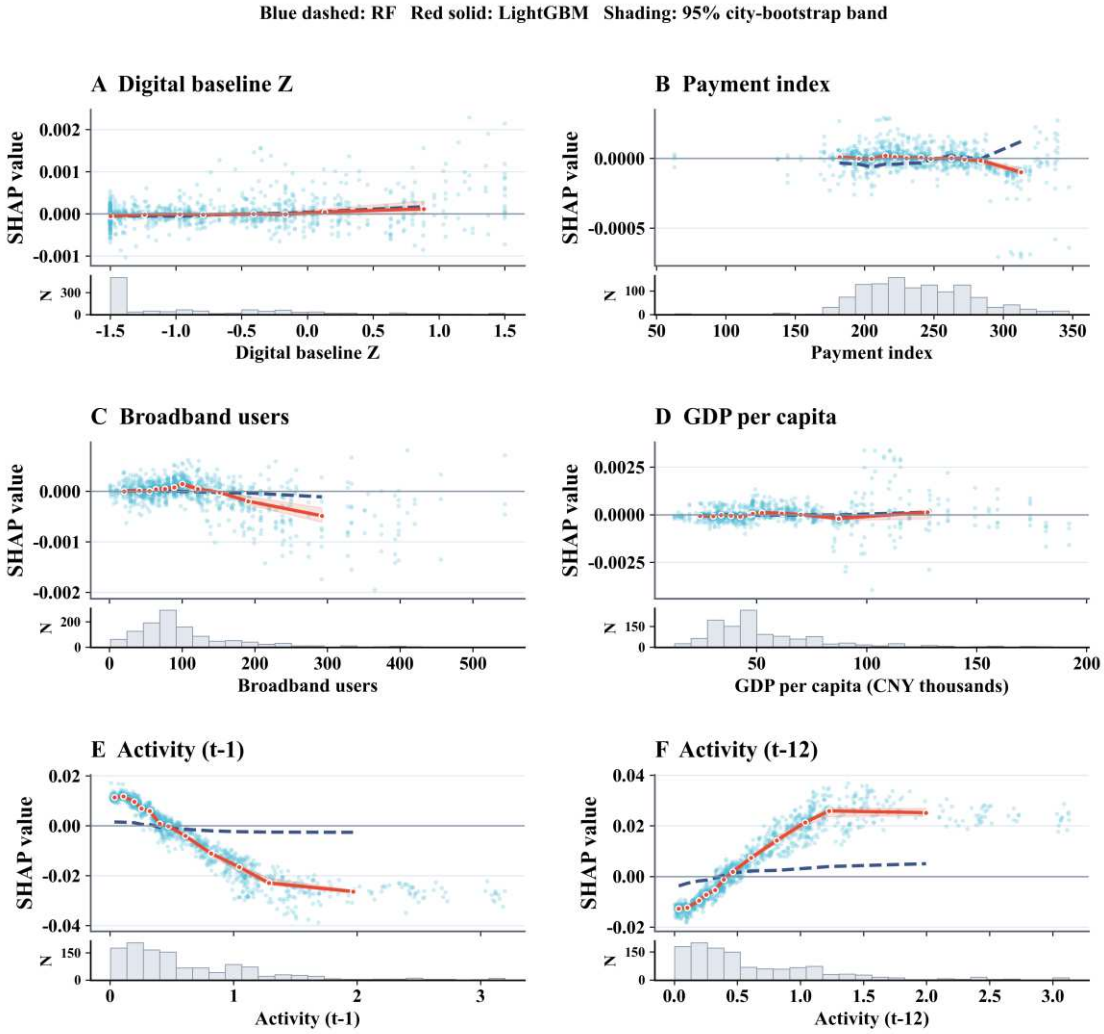


Figure 9 SHAP dependence for digital capacity, development, and historical activity

Note: Panels A–F show digital baseline *Z*, the payment index, broadband subscriptions, GDP per capita, and activity one month and twelve months earlier, respectively. Plotting conventions follow **Figure 8**. GDP per capita is measured in thousands of yuan.

4.4.4 Feature interactions

Figure 10 presents TreeSHAP interactions between extreme weather and digital payments, showing how predictive contributions vary across payment levels.

Digital payments reflect transaction-service infrastructure and adoption. Weather-related predictive differences across payment levels are consistent with heterogeneous adjustment capacity and complement the estimated distribution of policy-related buffering, without establishing a causal interaction.

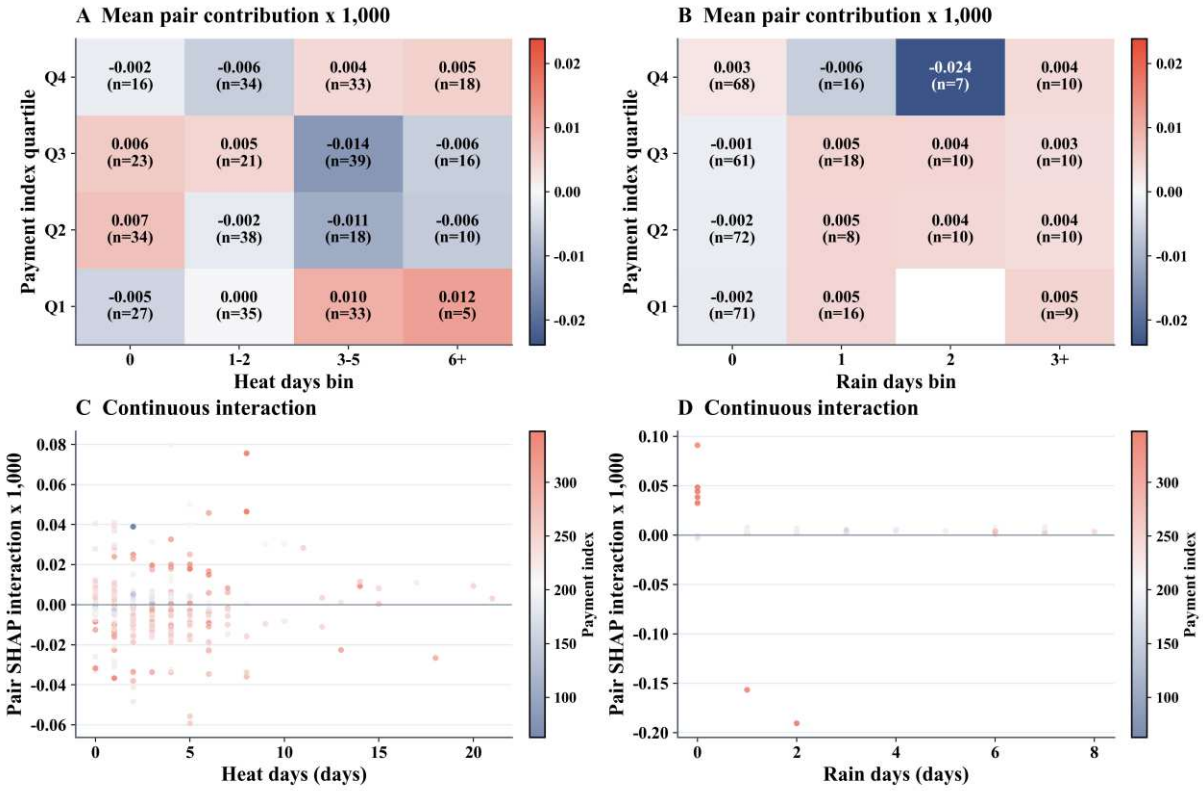


Figure 10 TreeSHAP interactions between weather and digital payments

Note: Panels A–B show mean interaction matrices for heat × payments and heavy rainfall × payments; Panels C–D show continuous scatterplots. The sample contains 400 test observations. Pairwise contributions equal twice the off-diagonal TreeSHAP values, and displayed values are multiplied by 1,000. Weather bins appear on the horizontal axes; payments are grouped into quartiles. Cells with $n < 5$ are omitted.

Figure 11 shows weather interactions with lagged economic activity, with predictive contributions varying across historical activity levels.

These patterns suggest that short-run weather responses depend partly on prior activity conditions, adding context to the weather–digital payment results.

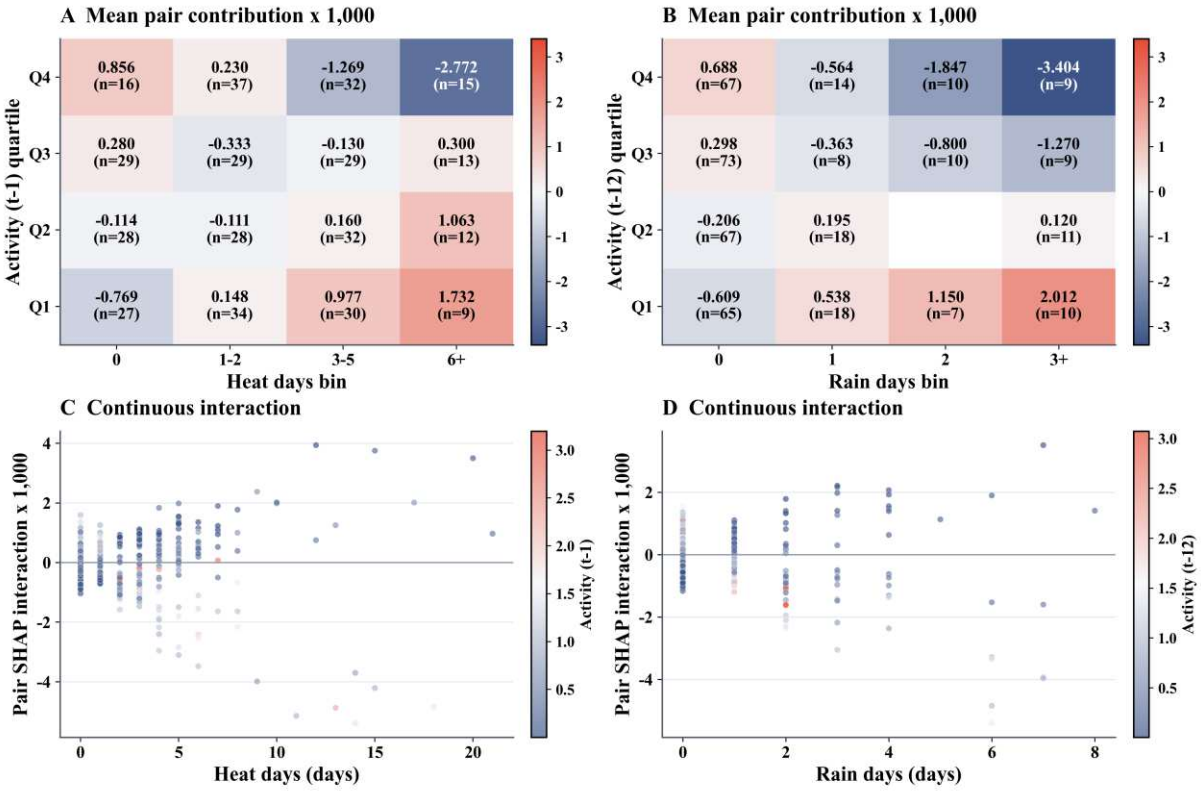


Figure 11 TreeSHAP interactions between weather and historical activity

Note: Panels A–B show interaction matrices combining weather with activity one month and twelve months earlier; Panels C–D show continuous scatterplots. The sample, weather bins, and display multiplier follow **Figure 10**. Activity is grouped into quartiles.

5 Discussion

5.1 Digitalization and urban climate resilience

The Information Consumption Demonstration City program reduces weather-related activity losses, extending evidence on temperature-related economic costs (Dell et al., 2012; Somanathan et al., 2021). Urban resilience depends not only on physical infrastructure but also on service organization and transaction continuity during shocks.

Lower information and transaction costs allow digital payments, online orders, and remote services to support market connections during disruptions (Goldfarb & Tucker, 2019). Increased service adoption after designation and its positive association with weather buffering underscore the importance of actual service use.

Buffering grows after designation and is concentrated around the shock month. Digital coordination can complement conventional disaster protection by facilitating timely service substitution and transaction continuity.

5.2 Unequal distribution of adaptation benefits

Table 4 and **Figure 5** show larger heat and rainfall buffering in cities with stronger initial digital capacity, including under fixed population weighting. Overall resilience gains can therefore coexist with unequal benefits across cities.

Existing payment networks and service platforms can accelerate the use of additional policy support, while user familiarity lowers switching costs during disruptions. Cities with weaker foundations may need greater investment in access and adoption to obtain comparable weather-buffering benefits.

Economic resources and infrastructure also shape adaptation. The persistent advantage under population weighting shows why digital policy should be evaluated for both aggregate buffering and the distribution of benefits across cities.

Improving access and effective digital-service use in less-connected cities can help extend adaptation benefits to more communities.

5.3 Policy implications and research limitations

The findings offer implications for coordinating digital policy with urban climate adaptation. First, digital services should be incorporated into adaptation systems, linking online payments, transaction information, public service appointments, and delivery coordination with emergency management. Continued operation during extreme weather also requires reliable communication, electricity, and logistics infrastructure. Better coordination between digital services and physical infrastructure can strengthen economic continuity.

Second, digital policy should give greater attention to actual service adoption in cities with weak digital foundations. In addition to expanding network and platform coverage, policy should improve access for small and medium-sized firms, lower residents' costs of using digital services, and strengthen digital skills and public service support. In cities with stronger digital foundations, priorities can shift toward service quality and effective accessibility across social groups, extending adaptation benefits to more economic actors.

Policy evaluation should also be broadened. Conventional assessments of digital development emphasize infrastructure scale, service coverage, and general economic growth. Our findings show that economic continuity during weather shocks also has value. Incorporating weather buffering, digital service adoption, and the distribution of adaptation benefits would provide a fuller assessment of the socioeconomic returns to digital development.

The analysis covers 20 newly designated cities and uses monthly nighttime lights. Future research could use firm- and household-level transactions to investigate within-city distributional effects and longer samples to assess interactions between digital services and physical infrastructure.

6 Conclusion

Using monthly data for 283 Chinese cities from 2017 to 2025 and the staggered designation of Information Consumption Demonstration Cities, this study examines how digital policy affects extreme-weather responses and the distribution of adaptation benefits. Digital policy significantly mitigates urban activity losses associated with heat and heavy rainfall. Post-policy buffering is consistent across models and robustness checks. Digital development improves routine economic activity and strengthens the capacity to maintain production, transactions, and services during adverse weather.

Adaptation benefits vary substantially with initial city conditions. Cities with stronger digital foundations obtain greater heat and rainfall buffering, and this advantage persists under fixed population weighting. Digital service adoption is positively associated with weather buffering, while economic development is also closely related to adaptation performance. Machine learning reveals nonlinear predictive relationships among weather exposure, historical activity, and initial city conditions, providing complementary evidence on short-run urban economic adjustment.

The study extends the assessment of digital policy from general economic promotion to urban climate adaptation and reveals an unequal distribution of benefits across cities. Urban policy should coordinate digital transformation with climate resilience, improving service accessibility and practical adoption in areas with weak digital foundations while strengthening overall adaptive capacity. This approach can broaden the climate adaptation benefits of digital development.

Author contributions: Conceptualization, Y.X.W. and Z.T.; methodology, Y.X.W. and Z.T.; software, Z.T.; validation, Y.Y.W., Y.X.W. and Z.T.; formal analysis, Z.T. and Y.X.W.; investigation, Z.T.; data curation, Z.T.; writing—original draft preparation, Y.X.W. and Z.T.; writing—review and editing, Y.Y.W., Y.X.W. and Z.T.; visualization, Z.T.; supervision, Y.Y.W.; project administration, Y.Y.W. All authors have read and agreed to the published version of the manuscript. Zhen Tan and Yangxin Wang contributed equally to this work and share first authorship.

Data availability: Detailed data and documentation are available in the Zenodo repository: https://zenodo.org/records/23456589.

Code availability: The code is available in the Zenodo repository: https://zenodo.org/records/23456589.

Competing Interest: The authors reported no potential conflict of interest.

Ethics declaration: Ethical approval was not required as no human participants were involved in this research.

Finding: This research did not receive any specific grant from funding agencies in the public, commercial, or not for-profit sectors.

Appendix A

Table A1 Event-bin estimates for activity levels and weather responses

Event bin	Estimate	SE	95% simultaneous CI	p
Level: months −36 to −25	0.00003	0.00136	[-0.00315, 0.00322]	0.982
Level: months −24 to −13	0.00014	0.00103	[-0.00225, 0.00254]	0.889
Level: months 0–11	0.01112***	0.00134	[0.00799, 0.01426]	<0.001
Level: months 12–23	0.00810***	0.00161	[0.00435, 0.01186]	<0.001
Heat: months −36 to −25	-0.00034	0.00037	[-0.00116, 0.00048]	0.353
Heat: months −24 to −13	-0.00031	0.00031	[-0.00101, 0.00039]	0.323
Heat: months 0–11	0.00132***	0.00033	[0.00058, 0.00207]	<0.001
Heat: months 12–23	0.00202***	0.00032	[0.00132, 0.00273]	<0.001
Rain: months −36 to −25	0.00003	0.00100	[-0.00227, 0.00233]	0.977
Rain: months −24 to −13	0.00018	0.00063	[-0.00126, 0.00162]	0.775
Rain: months 0–11	0.00214***	0.00068	[0.00058, 0.00370]	0.002
Rain: months 12–23	0.00318***	0.00061	[0.00178, 0.00459]	<0.001

Note: The reference period is months −12 to −3; months −2 and −1 are excluded. The 95% simultaneous intervals use 999 city-level score-multiplier draws. ***, **, and * indicate significance at the 1%, 5%, and 10% levels, respectively.

Table A2 Lead and placebo-date tests

Test	Result	Diagnostic	Sample
Level: joint leads	0.987	Not rejected	Main candidate sample
Heat: joint leads	0.596	Not rejected	Main candidate sample
Rain: joint leads	0.952	Not rejected	Main candidate sample
Policy level: placebo date	0.347	Not rejected	Pre-policy window only
Heat buffering: placebo date	0.769	Not rejected	Pre-policy window only
Rain buffering: placebo date	0.753	Not rejected	Pre-policy window only

Note: Lead entries report joint-test p-values. Placebo-date tests use only pre-policy windows.

Table A3 Group samples and fixed visibility conversions

Grouping	Weights	Lower/higher treated cities	Lower/higher mean q	Cities with valid weights
Digital capacity	Equal city weights	10 / 10	0.5944 / 0.7216	20
Digital capacity	Registered population	10 / 10	0.5988 / 0.7525	20
Weather exposure	Equal city weights	13 / 7	0.5992 / 0.7672	20
GDP per capita	Equal city weights	4 / 16	0.4835 / 0.7016	20

Note: Population weights are fixed at registered population in 2018. They change only the conversion of mean q within digital groups; the model is not refitted.

Table A4 Short-run lags and cumulative buffering

Weather	Lag	Estimate	SE	p
Heat	0	0.00197***	(0.00012)	<0.001
Heat	1	0.00060***	(0.00012)	<0.001
Heat	2	0.00026**	(0.00012)	0.026
Heat	3	0.00025	(0.00015)	0.101
Rain	0	0.00263***	(0.00027)	<0.001
Rain	1	0.00072***	(0.00026)	0.006
Rain	2	0.00040*	(0.00022)	0.072
Rain	3	0.00024	(0.00037)	0.504
Heat	Months 0–3 total	0.00308***	(0.00034)	<0.001
Rain	Months 0–3 total	0.00400***	(0.00042)	<0.001

Note: Cumulative effects sum activity deviations in the current month and months 1–3 and incorporate within-city covariance. ***, **, and * indicate significance at the 1%, 5%, and 10% levels, respectively.

Table A5 Machine learning feature definitions and processing

Feature group	Variables and figure labels	Count	Definition and processing
Current weather	Heat days / Rain days	2	P95 extreme heat days and heavy rain days

Feature group	Variables and figure labels	Count	Definition and processing
Current weather	Temperature / Rainfall anomaly	2	Monthly temperature and rainfall anomalies relative to the 1981–2010 baseline
Weather lags	Heat / Rain $(t-1, t-2, t-3)$	6	Lags 1–3 of each weather variable
Digital baseline	Digital baseline Z	1	Standardized 2018 payment index, fixed before treatment
Digital baseline	Payment index	1	Original 2018 digital payment index
Digital baseline	Broadband users	1	Original 2018 broadband subscriptions, in units of 10,000
Policy	Policy status	1	Policy status coded from designation timing
Measurement	NTL visibility	1	q, calculated from the 2018 mean of the original activity measure
Spatial	Longitude / Latitude	2	Longitude and latitude of the city representative point
Climate	Baseline temperature / rainfall	2	Annual temperature and precipitation in the 1981–2010 baseline
Development	GDP per capita	1	Original 2018 GDP per capita
Industry	Industry field	1	Original 2018 tertiary-industry field; anomalous measurement conventions require verification
Seasonality	Season sine / cosine	2	Sine and cosine encoding of calendar month
Past activity	Activity $(t-1, t-2, t-3, t-6, t-12)$	5	Selected lags of the urban activity level
Past changes	Change $(t-3)$	1	Third lag of monthly urban activity changes

Note: The models use 29 features. Imputation uses training-sample information only. The entirely missing resident-population column is excluded, and the contemporaneous service index is not included. Predictions are conditional on current weather and historical activity.

Table A6 Final machine learning parameters

Model	Parameter	Value
ElasticNet	alpha	0.0003
ElasticNet	l1_ratio	0.15
ElasticNet	max_iter	50000
ElasticNet	tol	1e-05
RandomForest	n_estimators	160
RandomForest	max_depth	14
RandomForest	min_samples_leaf	20
RandomForest	max_features	0.8
LightGBM	n_estimators	400
LightGBM	learning_rate	0.04
LightGBM	num_leaves	31
LightGBM	max_depth	-1
LightGBM	min_child_samples	70
LightGBM	colsample_bytree	0.9
LightGBM	reg_lambda	1

Note: Parameters are selected using validation RMSE for 2022–2023. The random seed is 20261006. The tree models share the same 29 features.

References

Adhvaryu, A., Kala, N., & Nyshadham, A. (2020). The light and the heat: Productivity co-benefits of energy-saving technology. *The Review of Economics and Statistics, 102*(4), 779–792. https://doi.org/10.1162/rest_a_00886

Akerman, A., Gaarder, I., & Mogstad, M. (2015). The skill complementarity of broadband internet. *The Quarterly Journal of Economics, 130*(4), 1781–1824. https://doi.org/10.1093/qje/qjv028

Athey, S., & Imbens, G. W. (2019). Machine learning methods that economists should know about. *Annual Review of Economics, 11*(1), 685–725. https://doi.org/10.1146/annurev-economics-080217-053433

Berrang-Ford, L., Siders, A. R., Lesnikowski, A., Fischer, A. P., Callaghan, M. W., Haddaway, N. R., Mach, K. J., Araos, M., Shah, M. A. R., Wannewitz, M., Doshi, D., Leiter, T., Matavel, C., Musah-Surugu, J. I., Wong-Parodi, G., Antwi-Agyei, P., Ajibade, I., Chauhan, N., Kakenmaster, W., … Abu, T. Z. (2021). A systematic global stocktake of evidence on human adaptation to climate change. *Nature Climate Change, 11*(11), 989–1000. https://doi.org/10.1038/s41558-021-01170-y

Bloom, N., Garicano, L., Sadun, R., & Van Reenen, J. (2014). The distinct effects of information technology and communication technology on firm organization. *Management Science, 60*(12), 2859–2885. https://doi.org/10.1287/mnsc.2014.2013

Bloom, N., Han, R., & Liang, J. (2024). Hybrid working from home improves retention without damaging performance. *Nature, 630*(8018), 920–925. https://doi.org/10.1038/s41586-024-07500-2

Breiman, L. (2001). Random forests. *Machine Learning, 45*(1), 5–32. https://doi.org/10.1023/a:1010933404324

Brynjolfsson, E., & Hitt, L. M. (2000). Beyond computation: Information technology, organizational transformation and business performance. *Journal of Economic Perspectives, 14*(4), 23–48. https://doi.org/10.1257/jep.14.4.23

Burke, M., Hsiang, S. M., & Miguel, E. (2015). Global non-linear effect of temperature on economic production. *Nature, 527*(7577), 235–239. https://doi.org/10.1038/nature15725

Callahan, C. W., & Mankin, J. S. (2022). Globally unequal effect of extreme heat on economic growth. *Science Advances, 8*(43), Article eadd3726. https://doi.org/10.1126/sciadv.add3726

Callaway, B., & Sant'Anna, P. H. C. (2021). Difference-in-differences with multiple time periods. *Journal of Econometrics, 225*(2), 200–230. https://doi.org/10.1016/j.jeconom.2020.12.001

Cameron, A. C., & Miller, D. L. (2015). A practitioner's guide to cluster-robust inference. *Journal of Human Resources, 50*(2), 317–372. https://doi.org/10.3368/jhr.50.2.317

Carleton, T. A., & Hsiang, S. M. (2016). Social and economic impacts of climate. *Science, 353*(6304), Article aad9837. https://doi.org/10.1126/science.aad9837

Chen, X., & Nordhaus, W. D. (2011). Using luminosity data as a proxy for economic statistics. *Proceedings of the National Academy of Sciences, 108*(21), 8589–8594. https://doi.org/10.1073/pnas.1017031108

Dell, M., Jones, B. F., & Olken, B. A. (2012). Temperature shocks and economic growth: Evidence from the last half century. *American Economic Journal: Macroeconomics, 4*(3), 66–95. https://doi.org/10.1257/mac.4.3.66

Dell, M., Jones, B. F., & Olken, B. A. (2014). What do we learn from the weather? The new climate-economy literature. *Journal of Economic Literature, 52*(3), 740–798. https://doi.org/10.1257/jel.52.3.740

Dingel, J. I., & Neiman, B. (2020). How many jobs can be done at home? *Journal of Public Economics, 189*, Article 104235. https://doi.org/10.1016/j.jpubeco.2020.104235

Dottori, F., Szewczyk, W., Ciscar, J.-C., Zhao, F., Alfieri, L., Hirabayashi, Y., Bianchi, A., Mongelli, I., Frieler, K., Betts, R. A., & Feyen, L. (2018). Increased human and economic losses from river flooding with anthropogenic warming. *Nature Climate Change, 8*(9), 781–786. https://doi.org/10.1038/s41558-018-0257-z

Eriksen, S., Schipper, E. L. F., Scoville-Simonds, M., Vincent, K., Adam, H. N., Brooks, N., Harding, B., Khatri, D., Lenaerts, L., Liverman, D., Mills-Novoa, M., Mosberg, M., Movik, S., Muok, B., Nightingale, A., Ojha, H., Sygna, L., Taylor, M., Vogel, C., & West, J. J. (2021). Adaptation interventions and their effect on vulnerability in developing countries: Help, hindrance or irrelevance? *World Development, 141*, Article 105383. https://doi.org/10.1016/j.worlddev.2020.105383

Forman, C., Goldfarb, A., & Greenstein, S. (2012). The Internet and local wages: A puzzle. *American Economic Review, 102*(1), 556–575. https://doi.org/10.1257/aer.102.1.556

Friedman, J. H. (2001). Greedy function approximation: A gradient boosting machine. *The Annals of Statistics, 29*(5), 1189–1232. https://doi.org/10.1214/aos/1013203451

Gelaro, R., McCarty, W., Suárez, M. J., Todling, R., Molod, A., Takacs, L., Randles, C. A., Darmenov, A., Bosilovich, M. G., Reichle, R., Wargan, K., Coy, L., Cullather, R., Draper, C., Akella, S., Buchard, V., Conaty, A., da Silva, A. M., Gu, W., … Zhao, B. (2017). The Modern-Era Retrospective Analysis for Research and Applications, Version 2 (MERRA-2). *Journal of Climate, 30*(14), 5419–5454. https://doi.org/10.1175/jcli-d-16-0758.1

Goldfarb, A., & Tucker, C. (2019). Digital economics. *Journal of Economic Literature, 57*(1), 3–43. https://doi.org/10.1257/jel.20171452

Goodman-Bacon, A. (2021). Difference-in-differences with variation in treatment timing. *Journal of Econometrics, 225*(2), 254–277. https://doi.org/10.1016/j.jeconom.2021.03.014

Graff Zivin, J., & Neidell, M. (2014). Temperature and the allocation of time: Implications for climate change. *Journal of Labor Economics, 32*(1), 1–26. https://doi.org/10.1086/671766

Henderson, J. V., Storeygard, A., & Weil, D. N. (2012). Measuring economic growth from outer space. *American Economic Review, 102*(2), 994–1028. https://doi.org/10.1257/aer.102.2.994

Hjort, J., & Poulsen, J. (2019). The arrival of fast internet and employment in Africa. *American Economic Review, 109*(3), 1032–1079. https://doi.org/10.1257/aer.20161385

Hong, B., Bonczak, B. J., Gupta, A., & Kontokosta, C. E. (2021). Measuring inequality in community resilience to natural disasters using large-scale mobility data. *Nature Communications, 12*(1), Article 1870. https://doi.org/10.1038/s41467-021-22160-w

Jack, W., & Suri, T. (2014). Risk sharing and transactions costs: Evidence from Kenya's mobile money revolution. *American Economic Review, 104*(1), 183–223. https://doi.org/10.1257/aer.104.1.183

Kotz, M., Levermann, A., & Wenz, L. (2022). The effect of rainfall changes on economic production. *Nature, 601*(7892), 223–227. https://doi.org/10.1038/s41586-021-04283-8

Kotz, M., Wenz, L., Stechemesser, A., Kalkuhl, M., & Levermann, A. (2021). Day-to-day temperature variability reduces economic growth. *Nature Climate Change, 11*(4), 319–325. https://doi.org/10.1038/s41558-020-00985-5

Li, Y., Svenning, J.-C., Zhou, W., Zhu, K., Abrams, J. F., Lenton, T. M., Ripple, W. J., Yu, Z., Teng, S. N., Dunn, R. R., & Xu, C. (2024). Green spaces provide substantial but unequal urban cooling globally. *Nature Communications, 15*(1), Article 7108. https://doi.org/10.1038/s41467-024-51355-0

Lundberg, S. M., Erion, G., Chen, H., DeGrave, A., Prutkin, J. M., Nair, B., Katz, R., Himmelfarb, J., Bansal, N., & Lee, S.-I. (2020). From local explanations to global understanding with explainable AI for trees. *Nature Machine Intelligence, 2*(1), 56–67. https://doi.org/10.1038/s42256-019-0138-9

Lythreatis, S., Singh, S. K., & El-Kassar, A.-N. (2022). The digital divide: A review and future research agenda. *Technological Forecasting and Social Change, 175*, Article 121359. https://doi.org/10.1016/j.techfore.2021.121359

Meerow, S., & Newell, J. P. (2019). Urban resilience for whom, what, when, where, and why? *Urban Geography, 40*(3), 309–329. https://doi.org/10.1080/02723638.2016.1206395

Meerow, S., Newell, J. P., & Stults, M. (2016). Defining urban resilience: A review. *Landscape and Urban Planning, 147*, 38–49. https://doi.org/10.1016/j.landurbplan.2015.11.011

Mullainathan, S., & Spiess, J. (2017). Machine learning: An applied econometric approach. *Journal of Economic Perspectives, 31*(2), 87–106. https://doi.org/10.1257/jep.31.2.87

Rambachan, A., & Roth, J. (2023). A more credible approach to parallel trends. *Review of Economic Studies, 90*(5), 2555–2591. https://doi.org/10.1093/restud/rdad018

Román, M. O., Wang, Z., Sun, Q., Kalb, V., Miller, S. D., Molthan, A., Schultz, L., Bell, J., Stokes, E. C., Pandey, B., Seto, K. C., Hall, D., Oda, T., Wolfe, R. E., Lin, G., Golpayegani, N., Devadiga, S., Davidson, C., Sarkar, S., … Masuoka, E. J. (2018). NASA's Black Marble nighttime lights product suite. *Remote Sensing of Environment, 210*, 113–143. https://doi.org/10.1016/j.rse.2018.03.017

Roth, J., Sant'Anna, P. H. C., Bilinski, A., & Poe, J. (2023). What's trending in difference-in-differences? A synthesis of the recent econometrics literature. *Journal of Econometrics, 235*(2), 2218–2244. https://doi.org/10.1016/j.jeconom.2023.03.008

Scheerder, A., van Deursen, A., & van Dijk, J. (2017). Determinants of Internet skills, uses and outcomes. A systematic review of the second- and third-level digital divide. *Telematics and Informatics, 34*(8), 1607–1624. https://doi.org/10.1016/j.tele.2017.07.007

Shi, L., Chu, E., Anguelovski, I., Aylett, A., Debats, J., Goh, K., Schenk, T., Seto, K. C., Dodman, D., Roberts, D., Roberts, J. T., & VanDeveer, S. D. (2016). Roadmap towards justice in urban climate adaptation research. *Nature Climate Change, 6*(2), 131–137. https://doi.org/10.1038/nclimate2841

Siders, A. R. (2019). Adaptive capacity to climate change: A synthesis of concepts, methods, and findings in a fragmented field. *WIREs Climate Change, 10*(3), Article e573. https://doi.org/10.1002/wcc.573

Somanathan, E., Somanathan, R., Sudarshan, A., & Tewari, M. (2021). The impact of temperature on productivity and labor supply: Evidence from Indian manufacturing. *Journal of Political Economy, 129*(6), 1797–1827. https://doi.org/10.1086/713733

Sun, L., & Abraham, S. (2021). Estimating dynamic treatment effects in event studies with heterogeneous treatment effects. *Journal of Econometrics, 225*(2), 175–199. https://doi.org/10.1016/j.jeconom.2020.09.006

Suri, T., & Jack, W. (2016). The long-run poverty and gender impacts of mobile money. *Science, 354*(6317), 1288–1292. https://doi.org/10.1126/science.aah5309

van Deursen, A. J. A. M., & van Dijk, J. A. G. M. (2019). The first-level digital divide shifts from inequalities in physical access to inequalities in material access. *New Media & Society, 21*(2), 354–375. https://doi.org/10.1177/1461444818797082

Verhoef, P. C., Broekhuizen, T., Bart, Y., Bhattacharya, A., Dong, J. Q., Fabian, N., & Haenlein, M. (2021). Digital transformation: A multidisciplinary reflection and research agenda. *Journal of Business Research, 122*, 889–901. https://doi.org/10.1016/j.jbusres.2019.09.022

Vial, G. (2019). Understanding digital transformation: A review and a research agenda. *The Journal of Strategic Information Systems, 28*(2), 118–144. https://doi.org/10.1016/j.jsis.2019.01.003

Xu, Q., Zhong, M., & Dong, Y. (2024). Digital economy and risk response: How the digital economy affects urban resilience. *Cities, 155*, Article 105397. https://doi.org/10.1016/j.cities.2024.105397

Zhang, P., Deschenes, O., Meng, K., & Zhang, J. (2018). Temperature effects on productivity and factor reallocation: Evidence from a half million Chinese manufacturing plants. *Journal of Environmental Economics and Management, 88*, 1–17. https://doi.org/10.1016/j.jeem.2017.11.001

Zou, H., & Hastie, T. (2005). Regularization and variable selection via the elastic net. *Journal of the Royal Statistical Society Series B: Statistical Methodology, 67*(2), 301–320. https://doi.org/10.1111/j.1467-9868.2005.00503.x

Supplementary Files

This is a list of supplementary files associated with this preprint. Click to download.

- CodeData.zip